DRAFT of the MODIS Level 1B Algorithm Theoretical Basis Document Version 2.0 [MOD-02]

May 1997

MCM-ATBD-01-U-DNCN

Prepared For:

National Aeronautics and Space Administration
Goddard Space Flight Center
Contract No. NAS5-32373
By: MODIS Characterization and Support Team

Prepared by:

Richard Barbieri — Date
SAIC/GSC MCST Task Leader

Reviewed by:

Harry Montgomery — Date
MCST Algorithm Development Team

Shiyue Qiu — Date
MCST Algorithm Development Team

Bob Barnes — Date
MCST Algorithm Development Team

Approved by:

Bruce Guenther — Date
MCST Project Manager

Vincent V. Salomonson — Date
MODIS Science Team Leader

1. INTRODUCTION, CONTEXT/SCOPE AND REFERENCE DOCUMENTS

The Moderate Resolution Imaging Spectroradiometer (MODIS) is a passive, imaging spectroradiometer carrying 490 detectors, arranged in 36 spectral bands that are sampled across the visible and infrared spectrum. It is a high signal-to-noise instrument designed to satisfy a diverse set of oceanographic, terrestrial and atmospheric science observational needs. The MODIS Characterization Support Team (MCST), working under the direction of the MODIS Team Leader, is responsible for developing the characterization and calibration of the MODIS instruments. This document describes the theoretical basis for the approach used to calibrate the instrument data stored in the MODIS Level 1B (MOD02) product.

The MODIS Level 1B algorithm describes how the data products are derived from the sensor digital number stream (Level 1A data). This Algorithm Theoretical Basis Document (ATBD) describes the algorithm, and thus defines the function of the software code that creates the Level 1B product. The characteristics of the algorithm to produce the top-of-the-atmosphere (at-sensor-aperture) radiance and reflectance products are determined by the components of the sensor design. The format of the document is:

1.1 Statement of Document Scope

This document describes the physical and engineering understanding of how MODIS will operate in space and it provides the equations implemented by the L1B software that, in turn, generates the MODIS MOD-02 data product. It is a summary document that presents the formulae and error budgets used to transform MODIS digital counts to radiance and reflectance. This document also describes the MODIS calibration and validation process. This document provides references to documents containing more complete derivations of results and to documents that explain the implementation of these algorithms as computer programs. This ATBD corresponds to the Version 2.0 software release.

At the time of development of this Version, analysis of the Engineering Model (EM) data has been completed. Thermal Vacuum testing of the Protoflight Model (PFM) that will go to orbit on the AM-1 spacecraft has not been completed and the data from those tests have not been analyzed and interpreted. Consequently, this Version is based on the (EM) instrument which in some aspects may be significantly different from the actual on-orbit sensor. In the context of this document, the MCST makes no distinction between instances where the EM testing and characterization was inconclusive to define sensor performance, and instances where the EM and PFM models perform differently.

An improved version of the Level 1B software, corresponding to an improved understanding of likely PFM performance on-orbit, will be developed and operated within the Compute Resources of MCST (CROM). This version will be improved immediately after launch as warranted, and used to produce Level 1B products for the early investigations of the Science Team. At the time that a high quality Level 1B product is available from the revised code, a Version 2.1 software delivery will be provided to the PGS through the MODIS Science Data Support Team (SDST). The MODIS Level 1B (MOD02) Data Product Specification is provided in Appendix F.

Data flow diagrams, program modules, and metadata are described fully in the MODIS Level 1B Software Design Document [Hopkins et al.1995b]. Summary data flow diagrams are provided for the Reflected Solar and Emissive infrared bands algorithms in Sections 3.1 and 3.2 of this document. Solar and lunar vector information from the MODIS Geolocation product is assumed within the L1B algorithm; a separate ATBD exists for the MODIS geolocation algorithms [Wolfe et al., 1995].

The basic strategy for making improvements to the product corresponds to improved understanding of the sensor performance. The contributions to this process expected from vicarious calibration is discussed in section 2.4. Specific instances where there is uncertainty

regarding sensor performance are reviewed in section 4. These are areas that MCST will watch carefully during the PFM thermal vacuum test data analysis.

1.2 The MOD-02 Data Product and its Role in MODIS Data Processing

The MOD-02 calibration data product results from the application of the formula and determination of corresponding uncertainties described in this document and the accompanying support documents. The support documents present the details of how the instrument data are transformed from counts to:

(1) effective digital numbers, DN*, radiances, and reflectance times cosine theta values, for the solar reflecting bands,
(2) radiances for the emissive bands,
(3) changes from prelaunch calibration of center wavelengths for the solar reflecting bands,
(4) relative spatial shifts of the pixels along scan and the bands along track.

Items (1) and (2) are the focus of this document and also the focus of the on line production processing efforts. They will be produced at the DAAC for all MODIS data. Items (3) and (4) are done off-line from the production processing. They will be produced with the CROM.

1.3 Relevant Documents

The parent documents of this document are [EOS, 1994] and [Salomonson, 1994]. Previous relevant publications include [Guenther et al., 1995], [King, 1994], [Weber, 1993], [SBRC, 1993], and [SBRC, 1994a]. Other applicable documents are listed in Appendix E.

2. OVERVIEW AND BACKGROUND INFORMATION

2.1 Experimental Objective

MODIS is the cornerstone instrument for the AM-1 spacecraft. The AM-1 spacecraft is scheduled to be launched in June 1998 into a 10:30 AM (descending node) orbit.

The near-daily coverage of MODIS, combined with its continuous operation, broad spectral coverage and relatively high spatial resolution, make the MODIS instrument central to the objective of EOS. MODIS data products will be provided by the MODIS Science Team in support of the Earth science community at large and the interdisciplinary investigators, as well MODIS Science Team members' own investigations. MODIS observations and data products will be applied to many of the areas identified as EOS science topics, such as:

* Land surface composition
* Land surface biological activity, phonology and physical state
* Surface temperature
* Snow and sea-ice extent and character
* Ocean and lake physics and biogeochemical activity
* Aerosol properties
* Cloud properties.

The data telemetered to the ground is 12 bits per pixel for all science on-board calibrators data. Half the orbit is in “day” mode, and half is in “night” mode. Day mode includes all 36 bands; night mode includes only bands 20 through 36. Data from all the on-board calibrators always are included in the telemetry stream.

2.2 Historical Perspective

MODIS is designed to continue observations for global climate change similar to those initiated with the Coastal Zone Color Scanner (CZCS), the Advance Very High Resolution Radiometer (AVHRR), the High Resolution Infrared Spectrometer (HIRS) and the Thematic Mapper (TM). Additional features that have been incorporated in the sensor include a thin-cirrus cloud detection channel, low gain bands to allow for surface-fire detection and high gain bands for ocean chlorophyll fluorescence-line height discrimination. Many of the MODIS science data products rely heavily on previous development from the precursor instruments.

2.3 Instrument Characteristics

MODIS has 36 spectral bands with center wavelengths ranging from 0.41 μm to 14.23 μm; these are listed in Appendix B, and they are depicted in Figure 1. The detector numbering convention in Figure 1 corresponds to that used by the instrument builder. 20 bands have a central wavelength below 2.2 μm and are known as reflected solar bands. The remaining 16 bands with a center wavelength greater than 3μm are known as emissive infrared bands. Two of the bands are imaged at a nominal resolution of 250m at nadir, five bands are imaged at 500m at nadir, and the remaining bands are imaged at 1000m at nadir. Bands 13 and 14 each have two gain settings, 13 low, 13 high, 14 low, and 14 high, telemetered from the instrument. All bands are telemetered at 12 bits.

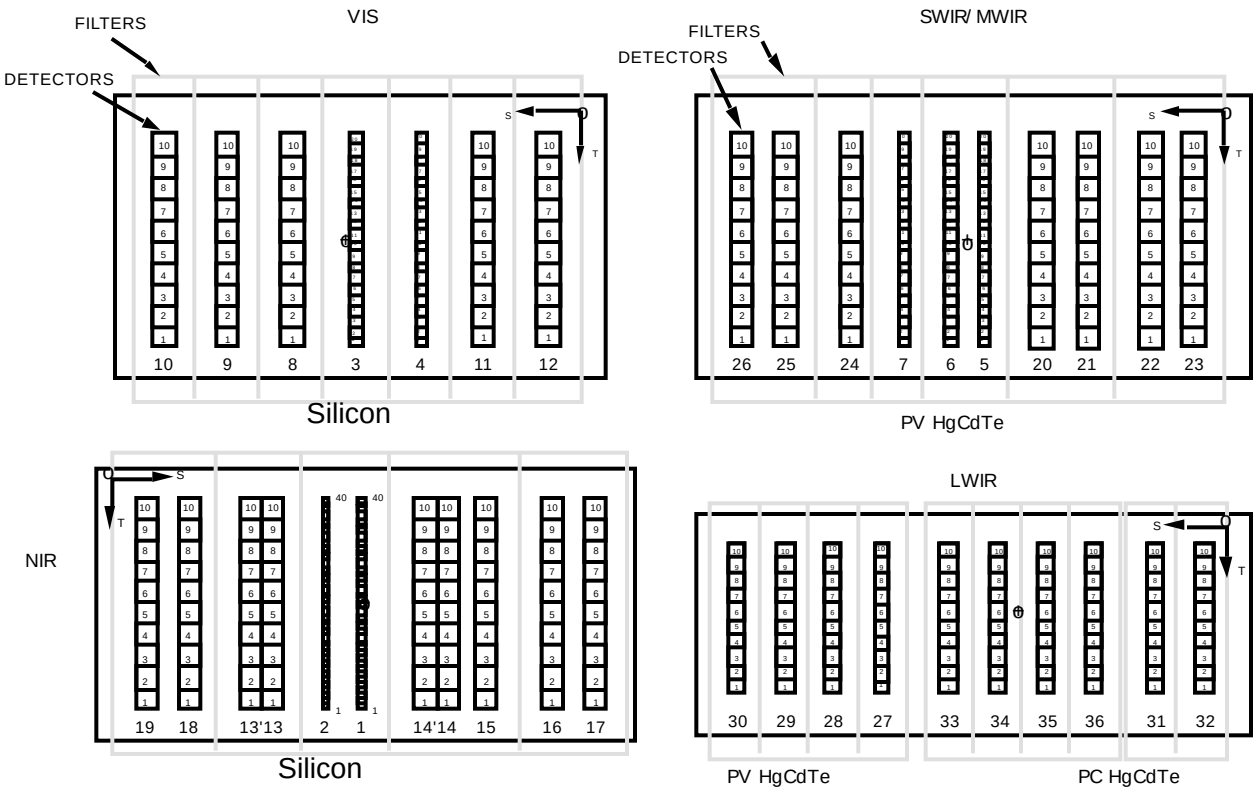

Figure 1: ***Focal Plane Assembly***

Bands 13 and 14 are time-delay-integration (TDI) bands. The low gain values for these bands results from the telemetry reading from a single frame. The high gain values for these bands results from the sum on-board from adjacent detectors pairs for each channel in each band.

Scene radiant flux reflects from the double sided, beryllium scan mirror, that is continuously rotating at 20.3 rpm with a period maintained to 0.001 sec so as to control scan to scan underlap. The mirror is oval shaped, 21 cm wide (the axis of rotation) and 58 cm long; it is nickel plated and coated with silver (Si O_x) for high reflectance and low scatter over the broad spectral range of the sensor and low polarization for center wavelengths below 1 μm. The reflectivity of the scan mirror is a function of the angle of incidence (AOI) of the scene energy onto the scan mirror.

Energy from the scan mirror impinges upon the afocal telescope assembly fold mirror and reflects into a plane perpendicular to the scan plane. The energy then strikes the primary mirror (the entrance pupil), goes through a field stop and then onto the secondary mirror. The mirrors are made of Zero-Dur low expansion substrates with protected silver coatings. The individual mirror elements are mounted onto a graphite-epoxy structure to maintain alignment of the elements. Immediately after the secondary mirror is a dichroic beamsplitter assembly (consisting of three beamsplitters) that directs the energy through four refractive objective assemblies and then onto the four focal plane assemblies (FPAs) with their individual bandpass filters.

The beamsplitters are used to achieve spectral separation, dividing the MODIS spectral domain into four spectral regions: visible (VIS) (0.4 to 0.6 μm), near infrared (NIR) (0.6 to 1.0 μm), short wavelength/medium wavelength infrared (SWIR/MWIR) (1.0 to 6 μm), and long wavelength infrared (LWIR) (6.0 to 14.5 μm). Dichroic 1 uses a ZnSe substrate and reflects the entire VIS, NIR region while transmitting the balance of the scene energy to 14. 5 μm . Dichroic 2 uses a BK-

7 substrate and reflects energy to the bands between 0.4 μm and 0.6 μm . Dichroic 3 also uses a ZnSe substrate and reflects energy to bands between 1 μm and 6 μm . Out-of-spectral-band rejection is accomplished through blocking filters on both bandpass filters and dichroic .

Spectral separation occurs at the FPAs with dielectric bandpass filters for each band. These filters are deposited on glass substrates; in some cases bandpass filters for two bands are deposited on a single substrate. The filter substrates are mounted to a common substrate mask, one per FPA. The mask provides some spectral out-of-band blocking as well as masking for the field-of-view of the detectors.

Low residual polarization sensitivity is required for bands between 0.43 μm and 2.2 μm . The requirement for less than 2% polarization from 0.43 μm to 2.2 μm is achieved by using silver coated scan and fold mirrors oriented in a crossed way. Low residual polarization sensitivity for the 0.41 μm band is desired also, but is not included in the sensor specification.

Each spectral region has an objective lens assembly for imaging scene energy onto the corresponding focal plane. On each focal plane are rows of detectors aligned in the along track direction so as to image 10 km in the track direction of the scene. Consequently there are 10 detectors along track in the 1000 m bands, 20 detectors along track in the 500 m bands, and 40 in the 250 m bands. The sampling rate and mirror rotation are coordinated to provide samples in the along scan direction that are contiguous. Both sides of the rotating scan mirror are used. The composite of all 36 bands coregistered to build the equivalent of a 1X10 km field of view is identified as a single frame. The sensor electronics holds bands in its buffer, and provides an output that already has the overlapping bands for the field of view stored together in the data pockets.

The VIS and NIR FPAs operate at ambient temperature and are composed of photovoltaic silicon hybrids for low noise readout and excellent electrical transient response performance. A HgCdTe photovoltaic hybrid detector are used for the SWIR/MWIR bands out to 10 μm and on the LWIR FPAs. The LWIR FPA includes six bands of photoconductive HgCdTe detectors for wavelengths beyond 10 μm because these offer better performance at 83K in this region.

The passive radiative cooler assembly is designed to passively cool the SWIR/MWIR and LWIR focal planes to a nominal operating temperature of 83K and an end-of-mission temperature of 85K. The cooler requires a 170 by 115 degree clear field of view to space and employs three stages of cooling to achieve the at launch operating temperature of 83K. A 4K margin allows for potential degradation over the mission life and temperature control. The cold stage assembly houses the SWIR/MWIR and LWIR focal plane assemblies. The intermediate cooler window will operate at approximately 130K on orbit.

There is an analog signal processing electronics unit that provides the primary clocks and an analog-to-digital conversion electronics unit to provide bias voltages for all the photovoltaic detectors, preamplification of the LWIR photoconductive detectors, and conversion of the analog signals to 12 bit digital signals.

As the MODIS mirror scans, energy from several On-Board Calibrators (OBC) is reflected into the telescope (see Figure 2). As the scan mirror rotates, the following events occur (see Figure 3a):

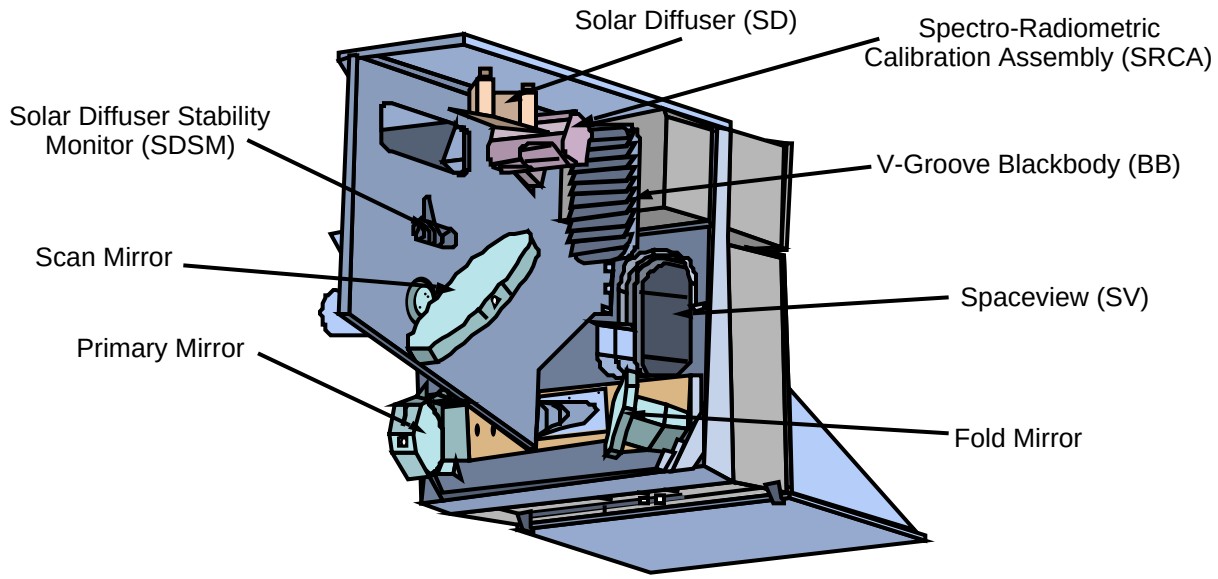

Figure 2: ***MODIS views a sequence of On-Board Calibrators.***

(1) The mirror scans the SD, (2) The mirror scans the SRCA, (3) The mirror scans the BB, (4) The mirror scans the SV port, and (5) The mirror scans the EV port. The data corresponding to measurements from the SD, the SRCA, the BB, the SV and the EV are identified individually as data sectors

Sector	# Frames Available	# Frames used in the L1B Code	Angle of Incidence of Light onto Scan Mirror for each Sector (degrees)
SD	50	the central 15	50.9-49.6
SRCA	10	10	38.4-38.1
BB	50	the central 15	27.3-26.6
SV	50	the central 15	11.6-10.9
EV	1354	1354	10.5-65.5

The order of the sectors described above is the order of the data in the Level 0 data stream and is the order of the scan mirror viewing. The targets for the SV and the EV are in the far field of the sensor and are in focus. The targets for the SD, SRCA, and the BB are in the near field and will be out of focus. The specific frames from a scan line which comprise the sector for each of the five targets may be altered by operational commands, changing either the entire (global) sector locations or the individual sector locations.

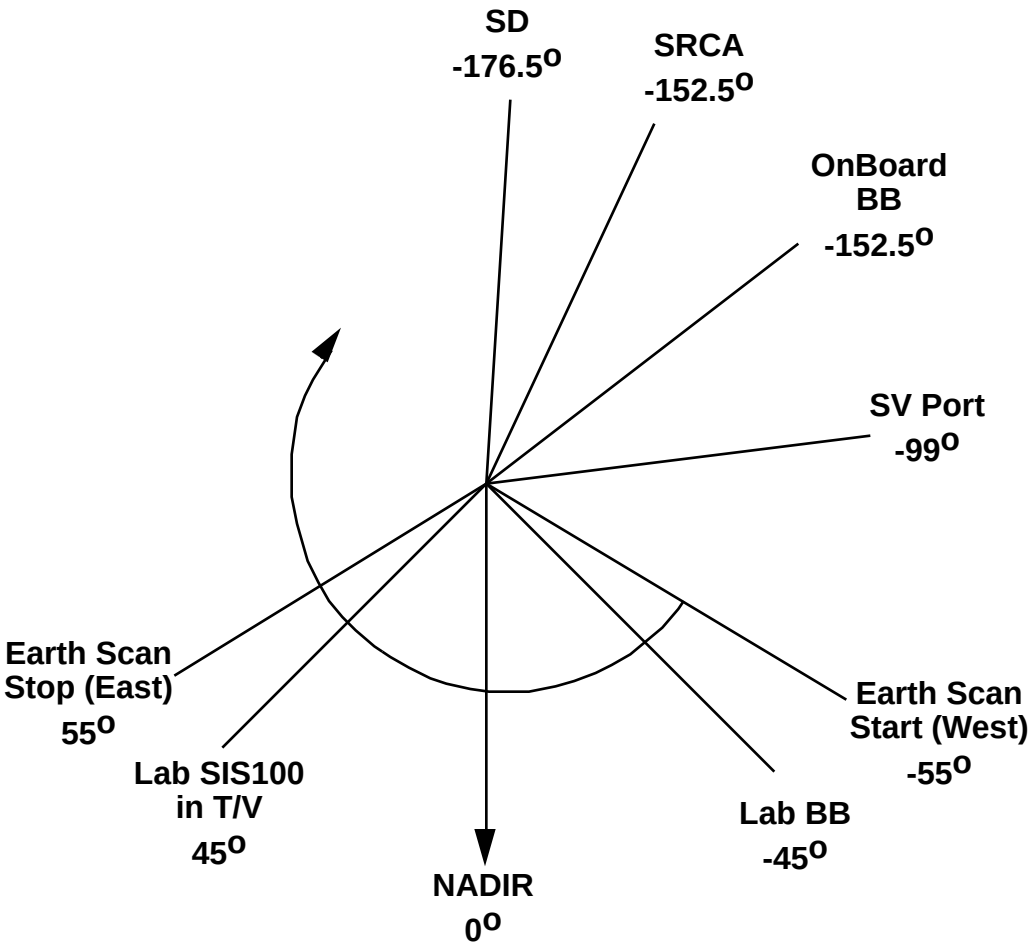

Figure 3a: ***As the MODIS Scan Mirror rotates, each side scans the Solar Diffuser, the Spectro-Radiometric Calibration Assembly, the blackbody, Space-and the Earth. The location of the primary ground calibration sources, in primary scan angle, also is shown.***

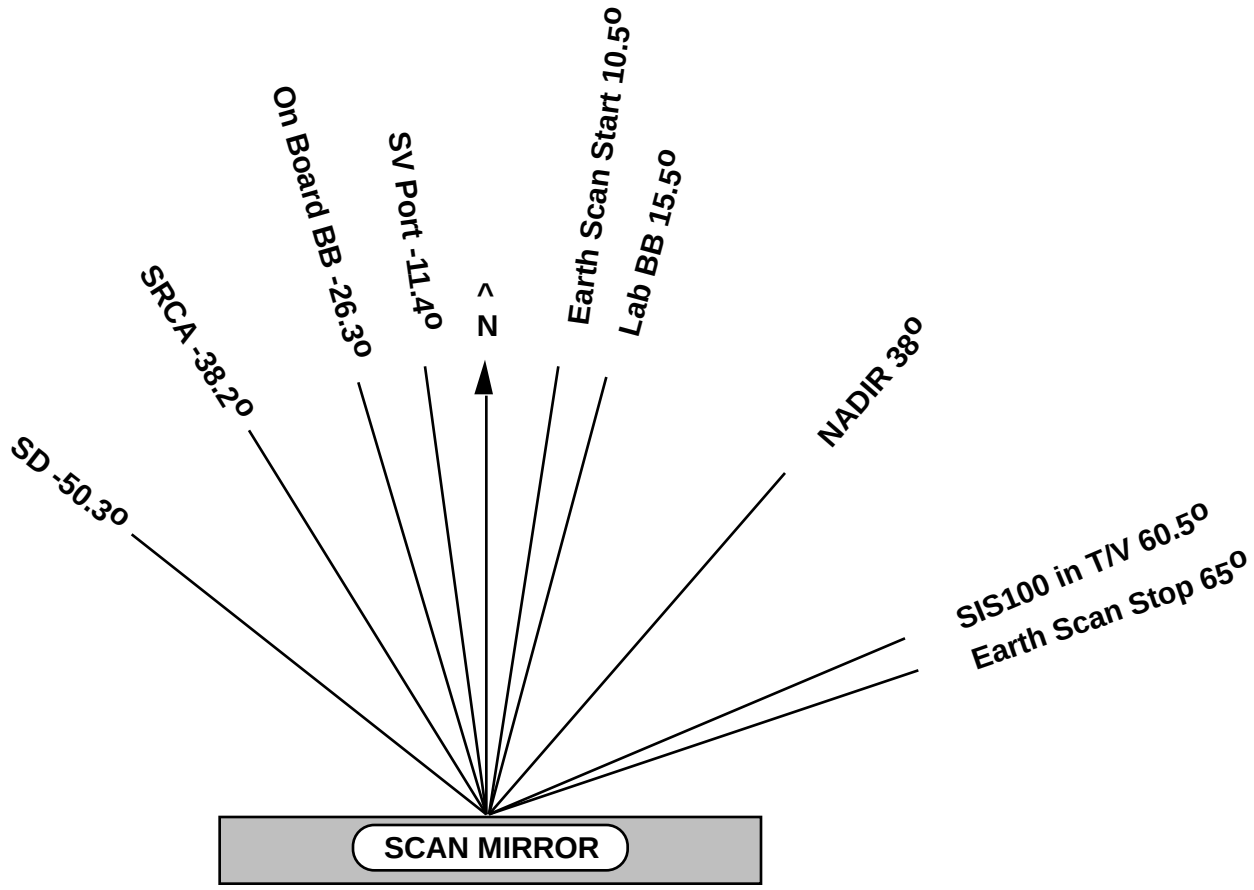

Figure 3b: ***The angle of incidence on the scan mirror which corresponds to each of the observed elements from Figure 3a is shown.***

The ground track direction is designated as the +x direction in instrument coordinate system; in the ground projection looking in the +x direction, the scan (which takes 0.45sec) moves from right to left orthogonal to the track direction. A swath (also known as a scan line) is 2200 km long, at nadir 10 km wide. A swath contains 1354 frames per scan; a frame contains ten 1km IFOVs in the track direction. MODIS is a paddle wheel scanner which has a bowtie characteristic at the scan edges, where the projection of the frame onto the earth enlarges to 3km by 20km with a rotated field of view.

The 250m bands (bands 1 & 2) have detector sizes that correspond to an Instantaneous Field of View (IFOV) of 250 m by 250 m. There are 40 detectors in the track direction and each detector is sampled four times within a frame.

The 500 m bands (bands 3-7) have detector sizes that correspond to an IFOV of 500 m by 500 m. There are 20 detectors in the track direction, and each detector is sampled two times within a frame.

In the L1B product, the ordering of the ten 1000m detectors within a band is such that detector 1 is at the trailing edge of the scan in the track direction and detector 10 is at the leading edge of the scan. A corresponding numbering scheme is used for the 500 m and 250 m bands. This convention in the Level 1B product is selected to allow easy use of Commercial-Off-The-Shelf (COTS) mapping software for product visualization and is the opposite of the detector number convention used by the instrument builder.

Spatial misalignments will be measured preflight at the SBRS, monitored in-flight by the SRCA and through image data analysis, and may be adjusted in-flight (focal plane-to-focal plane) by changing the sample start times individually for each focal plane. The best estimates of the sub-pixel offsets from nominal locations for each detector in each band will be included with the geolocation data products for use in subsequent processing.

2.3.1 On-Board Calibrators Characteristics

There are three On-Board Calibrators systems on MODIS:

- the Solar Diffuser and Solar Diffuser Stability Monitor (SD/SDSM),
- the SpectroRadiometric Calibration Assembly (SRCA),
- and the Black Body and space view (BB/SV).

In the Version 2.0 algorithm, only the BB/SV is used. The MCST scientists will learn after launch how to track changes in the MODIS sensitivity for the reflected solar bands with the SD/SDSM and include those approaches in a later version of the algorithm. The SRCA will be used for verification of the spectral characteristics on-orbit for the reflected solar bands, for the spatial coregistration of all bands, and for the long-term stability of MODIS reflected bands and electronics to the on-orbit thermal characteristics. For the SRCA products, the spectral and coregistration information will be included as part of the metadata associated with this product. Since each of these uses is a component of the Verification of the Level 1B product; these systems are described here. The complete description is provided in detailed support documents.

THE SOLAR DIFFUSER/SOLAR DIFFUSER STABILITY MONITOR (SD/SDSM)

The SD is a full aperture, end to end calibrator used to provide a measurement of sunlight for calibration of reflected solar bands. It consists of a spherical integrating source (SIS) with a input aperture and nine filtered detectors. Each filter has a narrow spectral bandpass so that the change in reflectance is effectively monitored at nine discrete wavelengths. When the AM platform is near the north pole and the SD door is open, the SD is fully illuminated by the Sun for approximately two minutes. Light is incident on the scan mirror at angles from 50.9 to 49.6 degrees for observations of the SD. During this period of time the SDSM is operated. The input aperture to the SDSM is filtered with a 2% transmission screen (perforated surface) which always is in place. The input aperture to the SD is filtered with a 8.5% transmission screen which can be deployed over the SD aperture by ground command. The SDSM detectors (housed in a miniature integrating sphere) alternately "see" an attenuated sun directly, sunlight scattered off the diffuser, and a dark internal screen to account for detector drifts. Degradation of the SD is tracked with the SDSM. The Earth scene beneath is in darkness during these measurements. Data acquired from the SD and from the SDSM are telemetered from the satellite regardless whether the sensor is operated in day or night mode.

SDSM Center Wavelengths (nm)								
412	469	531	555	645	748	858	905	940
Band 8	Band 3	Band 11	Band 4	Band 1	Band 15	Band 2	Band 17	Band 19

THE SPECTRORADIOMETRIC CALIBRATION ASSEMBLY (SRCA)

The SRCA is an end-to-end, partial aperture calibrator. It operates in three modes: spectral, radiometric, and spatial. In the spectral mode, instrument spectral response from 0.4 μm to 2.1 μm is tracked. In the spatial mode, instrument spatial band coregistration for all bands in both scan and track directions is tracked by using well defined reticules. In the radiometric mode reference radiometric levels are used to track changes in the radiometric calibration of MODIS through launch and to characterize the limits of within-orbit changes in responsivity for the reflected solar bands. The AOI range of the SRCA scan is 38.4 to 38.1 degrees. Sources within the SRCA are activated by ground command.

THE BLACK BODY/SPACE VIEW PORT (BB/SV)

The V-groove BB is a full aperture radiometric calibration source for the MWIR and LWIR bands. Temperature of the BB is known by twelve thermistors embedded in it. At the angle of view for MODIS, the emissivity of the BB is 0.993. It provides a known radiance source and is also used in the DC restore operation. The purpose of DC is to maintain the dynamic range within the specified limits as the instrument background changes due to instrument temperature changes. The BB provides one point on the calibration curve for each detector of the emissive bands. The BB is used for each scan line. The BB temperature is approximately isothermal with respect to the scan cavity. Internal BB heaters allow for operation of the blackbody at up to 315K. The AOI range of the BB is 27.3 to 26.6 degrees.

The space view port is an aperture in one of the electronic modules which permits a direct view of cold space. This view provides the zero reference points on the calibration curves for all 36 spectral bands. The SV is used for each scan line for each band. Approximately monthly the moon will be visible through the SV. During those times the moon will provide a radiance source for vicarious calibration rather than a zero radiance reference. The SV is used for scan mirror AOIs 11.6 to 10.9 degrees.

THE EARTH VIEW (EV) PORT

The double-sided scan mirror sweeps out a 110 degrees Earth field of view in each swath, effectively moving the instrument's ten spatial elements over a swath of the Earth 10 km wide at nadir. This scan width increases to 20 km at scan angles of +/- 55 degrees due to the panoramic "bow tie" effect. This effect leads to scan-to-scan overlap at scan angles greater than 25 degrees (actually, the 500 m and 250 m bands overlap at smaller scan angles, around 17 degrees for the 250 m bands). The AOI range of the EV is 10.5 to 65.5 degrees. The sampling interval is typically the amount of time it takes the projected image of a detector on the ground to move sideways (along-scan) one sample, 333.333 μsec for the 1 km bands.

2.4 The Calibration Timeline

2.4.1 Initial On-orbit Phase

The initial calibrations used for MODIS at launch will be the calibrations derived from the prelaunch calibration activities. The calibration for the reflective solar bands for radiance will be based on thermal vacuum measurements of the output of a spherical integrating sphere SIS(100). The calibration for the reflective solar bands for reflectance will be based on the laboratory measurements of the bi-directional reflectance distribution function of the flight solar diffuser. The

calibration for the emissive infrared bands will be based on thermal vacuum measurements of the output of a ground blackbody calibration source (BCS). Since the emissive infrared bands use the BB embedded in the instrument on each scan line, the calibration of the BB will be based on the ground blackbody calibration source. The BB emissivity will be "tuned" based on the BCS before launch.

Traceability of the radiance scale in the reflected solar bands to national standards will be through an irradiance lamp standard, which is the calibration standard for the spherical integrating source. Calibration of the radiance scale in the emissive infrared bands is through a temperature scale of the thermistors in the BCS. Validation of the radiance scales and the reflectance scales for the prelaunch values is being accomplished within the EOS round-robin programs conducted by the EOS Project Calibration Scientist. Round-robin measurements for emissive infrared bands have not begun at the time of this ATBD MOD02 Version 2.0 Document.

Spectral and spatial registration calibrations, as well as characterization of MODIS attributes are determined from prelaunch ambient laboratory testing, thermal vacuum testing, measurements of witness samples and in some cases modeling. The parameter listings Tables in Section 3 indicate the source of each parameter used in the algorithms. Parameters values are documented on the MCST home page of the World Wide Web.

2.4.2 Early On-orbit (Activation and Evaluation, A & E) Phase

This phase covers about the first three to six months of operations. Spatial co-registration will be checked using the SRCA in spatial mode. If the SRCA shows a shift in spatial registration from the prelaunch thermal vacuum testing, such a shift will be catalogued into the MCST Configuration Items List and therefore available to the science team on the MCST home page. These shifts will be reported in the data sets immediately.

Spectral band shape and center wavelength for the reflected solar bands will be checked using the SRCA in spectral mode. If the SRCA shows a shift in spectral registration that information will be incorporated into the MCST Configuration Items List and reported in the data sets immediately.

Radiometric calibration of the reflected solar bands will be checked using the SRCA in the radiometric mode. If the MODIS radiometric response to the SRCA shows a shift in the transfer to orbit such information will be noted and used later along with the interpretation of vicarious calibration data at the end stages of the A & E phase. Operation of the SRCA in radiometric mode during a full orbit will be used to validate sensor thermal/radiometric models. These thermal/radiometric models are likely to be adjusted immediately as a result of SRCA measurements and before vicarious calibration data sets are incorporated into the MODIS calibrations.

Changes in on-orbit radiometric performance within an orbit are checked by the SRCA. Such changes, if they occur, are most likely due to errors in understanding the temperature sensitivity of the detectors, optics, or electronics. Such changes will be incorporated into these algorithms immediately if any are discovered.

Changes in the radiometric calibration with time (days to weeks) will be checked with the solar diffuser measurements. Adjustments to the reflected solar band calibrations based on SD measurements are expected. These changes will not be incorporated before they are reviewed with the Science Team members and the major implications of the changes on the Level 2 algorithms are understood. By the end of the A&E period the earliest measurements which can be used as

vicarious calibration data for the Level 1B product are expected to be available. The most likely sources for this data include the land surface measurements from the University of Arizona (Slater, established for SPOT and TM data sets), ocean surface measurements from NOAA (Clark, established for the Ocean Color Temperature Sensor and perhaps SeaWiFS) and high altitude aircraft-borne spectrometer (Abel, established for AVHRR and GOES). All three of these data sets are for portions of the reflected solar bands, and none of them reach throughout the SWIR bands.

In addition, the A&E phase will establish the baseline trends used for monitoring the health of the instrument and the health of the data. These analyses will be performed in the CROM. Trending and monitoring will cover three basic categories. First, housekeeping telemetry will be monitored continuously to access the health of the instrument. This telemetry will be trended to allow the Instrument Operations Team predictive information about possible future problems. Second, the use of all potential limited life items will be tracked. These include SRCA bulb uses, motors, cooler cycles, and anything that might lead to changes in future operations in order to preserve functionality. Finally, the performance of the instrument will be trended to ensure that calibration is maintained over the life of the instrument. During the A&E phase, MCST will establish the initial trend lines for each of categories. These trend lines will be traced back to sensor performance during thermal vacuum testing.

Lunar observations will begin during this period. Research on the use of the lunar datasets is necessary, so they will be used for calibration no earlier than at the beginning the operational phase of the mission.

Reviews and workshops will be held at least every six months to brief the Science Team on sensor performance and calibration and characterization status. Each of these meetings will provide a set of recommendations for changes and improvements in the Level 1B product. The implementation of these recommendations is the responsibility of the head of the MODIS Characterization Support Team (MCST), under the direction of the MODIS Science Team Leader.

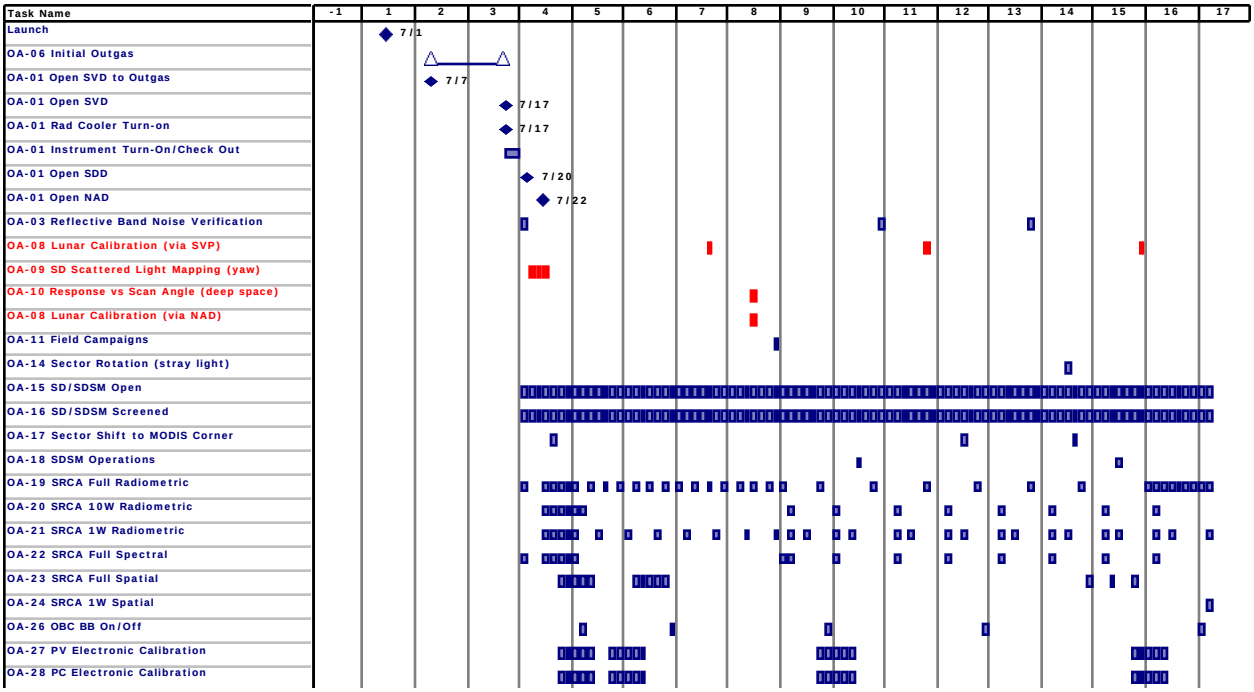

Figure 4: ***Activation and Evaluation Schedule***

2.4.3 Operational Phase

From six months after launch until the end of the MODIS mission, trending and monitoring of the primary data set, the engineering data set and the OBCs, validation, and updating calibration coefficients will be primary activities. Each of the MODIS discipline teams will conduct field campaigns, the MODIS calibration discipline group will continue vicarious calibration campaigns and aircraft underflights will be made. In addition, lunar radiometric calibration activities will be conducted through the SV port and perhaps through the EV port. Activities within the MCST are focused exclusively on improving the MODIS calibration and validating the L1B product.

3. ALGORITHM DESCRIPTION

Figure 5 provides a summary description of the primary calibration paths for the two MODIS science products for the reflected solar bands, the radiance and the reflectance product. The calibration tools which are either direct NIST standards or are subjects for the EOS/NIST round robin measurements programs are shown above the first dotted line in the Figure.

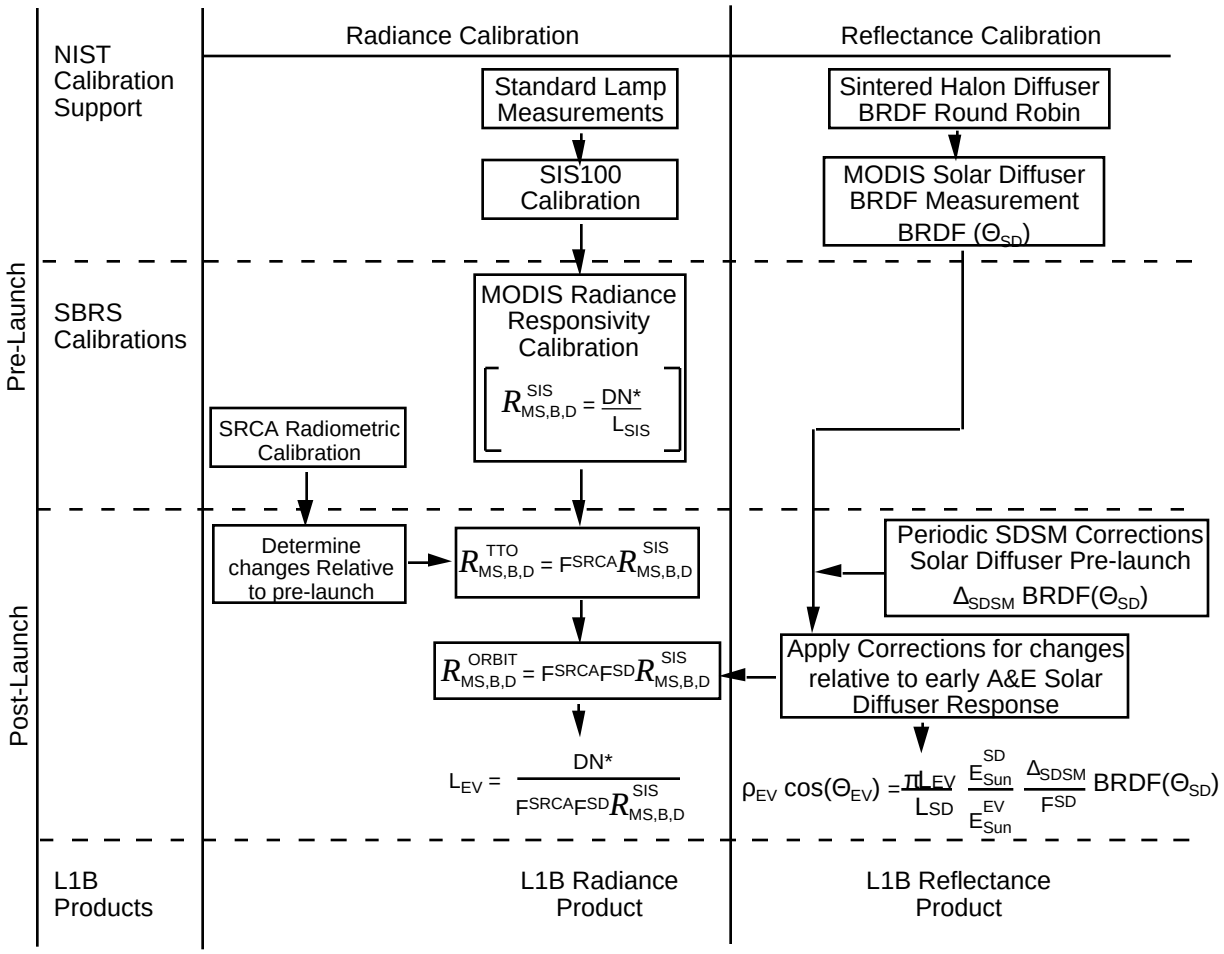

Figure 5: ***Reflective Calibration Paths***

3.1 The Reflected Solar Bands

For the reflected solar bands, the MODIS L1B algorithm has two principal data products. The first is the Earth-exiting spectral radiance for each band -- see Equation (7) in Section 3.1.2.1. This set of radiances is not normalized to 1 Astronomical Unit (1 AU) and will vary with the season due to changes of the Earth-sun distance. The units for spectral radiance are $\left[W\ m^{-2}\mu m^{-1}sr^{-1}\right]$. The second product is the Earth reflectance, see Equation (11) in Section 3.1.2.2, which will not vary with season due to changes in the Earth-sun distance. This reflectance is defined as the product of the Earth bi-directional reflectance factor, BRF_{EV}, multiplied by the cosine of the incidence angle of the solar flux at the Earth's surface (the solar zenith angle). The Earth reflectance is dimensionless.

Neither of these data products is derived using the absolute value for the solar irradiance. In other words, the MODIS radiances and reflectances are independent of any solar model. However, the band averaged solar irradiances for the reflected solar bands, using the compilation of Wehrli (1985), have been calculated and are available to data users as an auxiliary data product. They have been tabulated in one of the MODIS parameter lists and are available on the MCST home page.

The procedure for producing the emissive infrared radiometric product starts with the Level 1A digital numbers (12 Bits) and involves the operations defined by equation (7) to produce the calibrated radiances. These radiances are re-interpreted as 15 bit digital numbers and are coupled with gain and offset values which are stored in the metadata to provide coded radiance values. The product is stored in integer format to save on storage volume compared to floating point storage requirements. Bit 16 (MSB) is used as a quality flag.

3.1.1 Physics of the Problem

The initial on-orbit calibration for the reflected solar bands is the prelaunch laboratory calibration. The Level 1B output products from MODIS, on a pixel-by-pixel basis, are digital counts. For radiances from the solar bands, the basic measurement equation is

$$L_{EV,B,D} = \frac{DN_{EV,B,D}}{{}_{L,B,D}(t)} \qquad (1)$$

where

B	MODIS Band
D	Detector within band B
$L_{EV,B,D}$	Band-averaged spectral radiance from the Earth scene $\left[W\ m^{-2}\mu m^{-1}sr^{-1}\right]$
$DN_{EV,B,D}$	Effective digital counts from the detector (see Equation (6))
${}_{L,B,D}(t)$	Radiance responsivity from the calibration of MODIS $\left[counts W^{-1}m^{2}\mu m sr\right]$
t	Time after the start of on-orbit operations
L	as a subscript is used to identify these parameters as belonging to the radiance product calculations
$L_{EV,B,D}$,	as used by MODIS, is the band-averaged spectral radiance. It is defined by the equation

$$L_{EV,B,D} = \frac{\int_{\lambda_1}^{\lambda_2} L_{\lambda,EV} R_{\lambda,B,D} d\lambda}{\int_{\lambda_1}^{\lambda_2} R_{\lambda,B,D} d\lambda} \quad (2)$$

where

$L_{\lambda,EV}$	Spectral radiance of the Earth scene at wavelength λ $\left[W\ m^{-2}\mu m^{-1} sr^{-1}\right]$
$R_{\lambda,B,D}$	Relative spectral response at wavelength λ
λ_1 and λ_2	Wavelength range over which the detector has a significant quantum efficiency

The effective digital counts, $DN^*_{EV,B,D}$, are the raw counts from MODIS, corrected for zero offset and for instrument characteristics determined during calibration and characterization in the laboratory. The effective digital counts correct for on-orbit differences in the instrument from those under laboratory (calibration) conditions. For example, there is a correction for the difference between the temperature of the focal plane on orbit and that during calibration. In addition, the scan angle corrections for the solar bands are normalized to unity at the primary scan angle of 45°. This is the angle that the SIS(100) sits during the primary calibrations in thermal vacuum and is at 60.5° angle of incidence on the scan mirror. These corrections are discussed in Section 3.1.2.1.

The radiance responsivity, $^*_{L,B,D}$, is the radiance calibration factor for MODIS. This factor has three components. The first comes from the prelaunch radiometric calibration in the laboratory. The second comes from measurements that monitor relative changes in the responsivity of MODIS during the time interval between the laboratory calibration and the start of on-orbit operations, that is, during the transfer to orbit. And the third comes from measurements that monitor relative changes in the responsivity of the instrument during the lifetime of the mission. For MODIS, there is only one absolute measurement of responsivity. This is the laboratory calibration. The two other components are measures of the relative changes in responsivity.

For the first factor, the laboratory calibration uses an integrating sphere as a known radiance source to calculate the responsivity of each detector at several radiance levels

$$^*_{CAL,LB,D} = \frac{DN^*_{CAL,B,D}}{L_{CALB,D}} \quad (3)$$

and $^*_{CAL,LB,D}$ is calculated as the slope of a linear fitted curve of $DN^*_{CAL,B,D}$ versus $L_{CAL,B,D}$ for the set of calibration measurements. The calculation of the effective digital counts includes a correction for any non-linearity in the laboratory calibration (see Section 3.1.2.1).

For the second factor, the best estimate of the fractional change in responsivity during the transfer to orbit, $F_{TTO,L,B,D}$, is estimated from measurements from several sources. There is no procedure to automatically apply the transfer to orbit correction. Within MODIS, the SRCA will monitor instrument changes. In addition, initial measurements from the SD/SDSM will provide further information about instrument changes. Combined with measurements from lunar and other vicarious measurements, these data will be used to obtain an understanding of the instrument

responsivity at the start of on-orbit operations. The transfer to orbit correction, $F_{TTO,L,B,D}$, will be applied, as described in the Calibration Timeline in Section 2.4. The decision to implement this correction will derive from an internal MODIS review process. With the application of the transfer to orbit correction, the at launch responsivity of the MODIS reflected solar bands in equation (1) becomes

$$_{L,B,D}(0) = \quad _{CAL,L,B,D} F_{TTO,L,B,D} \tag{4}$$

For the third factor, changes in the responsivity of the reflected solar bands are monitored after the start of on-orbit operations. During A&E, MODIS will make an initial set of solar measurements with the SD/SDSM. After this time, the SD/SDSM will be used to monitor relative changes in the responsivities of the reflected solar bands. This diffuser-based responsivity correction, $F_{SDSM,L,B,D}(t)$, will be initialized to unity at launch, and the correction algorithm will operate off-line. This correction will be used for long-term changes in the responsivities of the reflected solar bands, that is, for changes over intervals from weeks to years. $F_{SDSM,L,B,D}(t)$ will be applied, as described in the Calibration Timeline in Section 2.4. The SD/SDSM are described in a detailed design document.

The SRCA for MODIS has been designed, among other things, to monitor instrument changes within an orbit. These intra-orbit variations may be caused by instrument temperature changes as the spacecraft passes through the sunlit and dark portions of the orbit or by other factors. The SRCA correction, $F_{SRCA,L,B,D}(t)$, will be used for changes that occur over the time interval of a single orbit. At launch, the SRCA correction will be initialized to unity. If instrument changes within an orbit are found, this correction will be applied immediately. A functional description of the SRCA is given in a detailed design document.

The radiance calibration factor from vicarious data, $F_{VC,L,B,D}(t)$, is a means of incorporating the results of satellite, aircraft, and surfaced-based measurements into the calibration of MODIS on orbit. This factor will be set to unity at launch. MODIS also will make a long-term set of measurements of reflected sunlight from the lunar surface. The correction factor from these measurements, $F_{LUNAR,L,B,D}(t)$, is separated from other vicarious measurements due to its nature as a long-term data set (that can last as long as the EOS mission) with frequently repeated measurements (several times a year). Again, $F_{VC,L,B,D}(t)$ and $F_{LUNAR,L,B,D}(t)$ will be applied according to the Calibration Timeline in Section 2.4. And both $F_{VC,L,B,D}(t)$ and $F_{LUNAR,L,B,D}(t)$ will have a time scale of a few months to several years.

With the inclusion of the correction terms for the SD/SDSM, SRCA, vicarious, and lunar measurements, the radiance responsivity term from equation (1) becomes

$$_{L,B,D}(t) = \quad _{CAL,L,B,D}(t) F_{TTO,L,B,D} \left\{ F_{SDSM,L,B,D}(t) F_{SRCA,L,B,D}(t) F_{VC,L,B,D}(t) F_{LUNAR,L,B,D}(t) \right\} \tag{5}$$

The most likely benefit from vicarious calibration is to identify either an error in the prelaunch calibration scale embodied in $^{*}_{CAL,L,B,D}$ or an error in our assessment of the changes in MODIS due to the rocket launch and orbit insertion, $F_{TTO,L,B,D}$. Consequently, in the final application of Equation (5),we expect to actually apportion identified errors amongst the terms $^{*}_{CAL}$ and F_{VC}, and will not handle this equation as if it is a multiplication of independent and orthogonal terms within the brackets.

Normalization for differences in responsivity detector-by-detector within each band will be obtained by observations of sunlight scattered off the solar diffuser. This correction will be incorporated into $_{CAL,B,D}$ in Equation (3).

3.1.2 Mathematical Description of the Algorithm

3.1.2.1 Effective Digital Counts and the Radiance Calculation

There are corrections to the MODIS digital counts based on the analysis of EM data. Additional corrections are expected after PFM testing, analyses, and interpretation.

In the reflected solar bands, the radiance and reflectance calibration algorithm corrects for systematic effects due to focal plane temperature, mirror side, scan angle, and non-linearity in the detector electronics and A/D converters. These corrections will apply to all radiance sources, including the radiance from the SRCA, SD, and EV. Whether the moon is visible in the SV port or not, the SV also will have the complete set of corrections applied. The following corrections are applied to each reflected solar band and detector for each scan line:

(1) Correct digital numbers for nonlinearity effects.
Five analog-to-digital (A/D) converters are used to generate the digital numbers (DN) from the MODIS focal planes. There are numerous instances of redundant electronic subsystems, and they are identified as Side A and Side B. Each will have separate characterization parameters, and changes in the case of Side A and Side B components are identified in the non-searchable metadata at the granule level. Indices for the Electrics Redundancy Vector are suppressed throughout this ATBD. Prelaunch laboratory testing demonstrates characterization of the deviation of each A/D from linearity, including a fixed pattern noise based on the total number bits that are on (high state). In addition, MODIS has an internal electronic calibration, called ECAL, which injects a series of voltages in the form of an electronic ramp immediately after the current-to-voltage converter for each detector. These voltages are paired with the digital counts from the detector. ECAL has been designed to determine the linearity in the intermediate amplifiers and A/D converter for each detector. Finally, the linearity of the MODIS measurements, from the detector to the digital output will be measured with the SIS(100) using several radiance levels. Of course, ECAL non-linearity must be quantified before the correction for each detector can be applied. An individual measurement DN then is corrected for the electronic non-linearity and fixed pattern noise through the use of a look-up table, designated Q, such that $DN'_{B,D} = DN\left[Q(B, DN_{B,D})\right]$. DN', then, is the expected response when corrected for non-linearities. The expected uncertainty in $DN'_{B,D}$ is 0.2%.

(2) Correct for zero radiance response
Every scan line includes a measurement of cold space and provides the detector zero radiance offset. Measurements of each scene must be corrected for zero radiance offsets. Each $DN'_{B,D}$ measured at the space view port is subject to the linearization filter described in (1) above and is designated $(DN'_{B,D})_{SV}$ such that $(DN'_{B,D})_{SV} = DN_{B,D}\left[Q(B, DN_{B,D})\right]_{SV}$ so that the signal from any scene with a measured $DN_{B,D}$ will be represented by $DN'_{B,D} - (DN'_{B,D})_{SV}$ for the linearized system. This correction is applied to Earth-view, solar diffuser, and SRCA data. When the moon is in the space view port, $(DN'_{B,D})_{SV}$ does not represent a response to zero radiance, and an alternative correction for zero radiance response must be applied.

(3) Correct measured DN for focal plane temperature effects
A linear correction is applied for the difference between a reference or calibration temperature, $T_{CAL}(FP_B)$, of a focal plane and the average focal plane temperature, $<T(FP_B)>$, where FP_B is the focal plane for band B. The temperature coefficient, $K_{B,D}$, is determined for each MODIS detector, with the determination based on responsivity variations observed during thermal vacuum testing. The magnitude of the temperature coefficient should range from about 0.01% to about 0.1% per degree. Within an orbit, the temperature of the uncooled VIS and NIR focal planes is expected to change by about one to two degrees. The uncertainty in the short-term temperature correction is expected to be very small. Over the life of the mission, MODIS will warm by ten or more degrees as the thermal blankets lose efficiency. For the reflected solar bands, any deficiency in this correction will become part of the long-term responsivity change. The uncertainties in this correction are expected to average about 0.2% for the reflected solar bands.

(4) Correct measured DN for scan angle effects
The mirror reflectance depends on the angle at which the mirror is viewed. The reference for this is the scan angle at which the SIS(100) is used for calibration during thermal vacuum testing (see Figures 3a,3b). The correction is applied through a lookup table $S(B,MS,F_{AOI})$ that includes differences in the reflectances of the two sides of the scan mirror, where MS=mirror side. The lunar, SRCA, and SD data segments are used at the scan mirror angle of incidence for that observation. Side-to-side differences in the scan mirror reflectivity will be substantially less than 1%, particularly near nadir. For the reflected solar bands, the reflectivity of the mirror can change by up to 3% for measurements near the edge of the swath. Again, it is estimated that the corrections in the L1B algorithm will reduce these uncertainties by a factor of five.

After these corrections have been applied, the notation for the uncorrected digital counts is changed to DN^*, known as effective digital counts. These counts are, in effect, those that the instrument would be expected to produce under laboratory conditions. DN^* is part of the process of carrying the laboratory calibration to the scene that MODIS views on orbit.

The complete correction from DN to effective DN, DN^*, is

$$DN_{B,D} = \left[DN'_{B,D} S(B,D,MS,F_{AOI}) - (DN'_{B,D})_{SV} S(B,D,MS,F_{AOI})_{SV} \right] \cdot \left\{ 1 + K_{B,D} \left[T(FP_B) - T_{CAL}(FP_B) \right] \right\} \quad (6)$$

When effective Earth-view digital counts from Equation (6) are combined with the radiance responsivity from equation (5), the radiances from the MODIS reflected solar bands are calculated from the basic measurement equation

$$L_{EV,B,D} = \frac{DN_{EV,B,D}}{{}_{L,B,D}(t_{EV})} \quad (7)$$

The practical considerations for the reflected solar bands portion of the L1B algorithm are found in Section 3.3.

3.1.2.2 Reflectance Calculation

In addition to its function as a radiometer, MODIS will be used on orbit as a reflectometer. In this mode, MODIS will act as a transfer radiometer between two diffuse reflecting surfaces, the SD and

the Earth. Both the SD and the Earth atmosphere system are reflecting surfaces, and the MODIS signal, when viewing these targets, results from the reflection of incident sunlight. MODIS uses the SD as a reference sample.

The preflight laboratory characterization of the diffuser determines its reflectance properties, that is, its radiance to irradiance reflectance ratio, using a NIST-characterized reference diffuser. Here, the ratio is called the solar diffuser bi-directional reflectance factor (BRF), ρ_{SD}. The BRF is a fundamental part of the definition of the MODIS reflectance product: the Earth bi-directional reflectance factor at multiplied by the cosine of the solar incidence angle. The BRF and the bi-directional reflectance distribution function (BRDF) are related by a factor of π steradians. The BRF is the greater of the two and is dimensionless. Reflectance is defined in terms of the BRDF, and the value of π in Equation (9) converts the BRDF to BRF.

There is no prelaunch solar calibration of the SD system, only a prelaunch BRF characterization, $\rho_{0,B,D}$. In addition, there is no method to monitor changes in this characterization from the laboratory to orbit. However, as with the radiance responsivity in section 3.1.2.1, there will be methods to monitor diffuser changes on orbit. Thus, the BRF of the SD at the time of each solar measurement, t_{SD}, is defined as

$$\rho_{SD,B,D}(t_{SD}) = \rho_{0,B,D}\left\{ F_{SDSM,\rho,B,D}(t_{SD}) F_{SRCA,\rho,B,D}(t_{SD}) F_{VC,\rho,B,D}(t_{SD}) F_{LUNAR,\rho,B,D}(t_{SD}) \right\} \quad (8)$$

ρ as a subscript is used to identify these parameters are belonging to the reflectances product calculations

The form of Equation (8) parallels that for Equation (5) in Section 3.1.2.1, and the correction factors in Equation (8) are analogs to the corresponding factors in that equation. The corrections in Equation (8) will be applied as described in the Calibration Timeline in Section 2.4. The difference between Equation (5) and Equation (8) is that there is no F_{TTO} correction, and the bracketed expression closely resembles the multiplication of orthogonal terms.

In a practical sense, the SDSM is the principal means of monitoring $\rho_{SD,B,D}(t_{SD})$. This is the task for which the SDSM was designed and built. If there are problems in determining the long-term changes in the SD using the SDSM, then these are symptoms of additional problems within the instrument. In those sections, $\rho_{0,B,D}$, is referred to as $BRF_{0,B}$.

On orbit, both the SD and the Earth will be illuminated by the same irradiance source. For the MODIS solar diffuser, the reflectance is given by

$$\rho_{SD,B,D}(t_{SD}) = \frac{\pi\, L_{SD,B,D}}{E_{SUN,B,D}\cos(\theta_{SD})} \quad (9)$$

where

$L_{SD,B,D}$ Spectral radiance from the diffuser measurement for detector, D, of band, B as determined from Equation (7) $\left[W\ m^{-2}\mu m^{-1} sr^{-1}\right]$

$\rho_{SD,B,D}$ Bi-directional reflectance factor of detector, D, band, B, at the time of the solar measurement [dimensionless],

$E_{SUN,B,D}$ Solar irradiance for detector, D, of band, B, for an Earth-sun distance at the "moment" this measurement is made. This parameter is determined by Equation (9) and equally well could be named $E_{MODIS,B,D}(t)\left[Wm^{-2}\mu m^{-1}\right]$

θ_{SD} Solar zenith angle relative to the normal to the SD surface

The term $\cos(\theta_{SD})$ accounts for the geometric expansion of the irradiance beam for angles other than normal incidence to the diffuser surface. It is used, since the solar image on the diffuser overfills the field of view of the MODIS measurement. In this presentation, the indices for the elevation and azimuth angles for incidence and reflectance are not shown here to simplify the equations. It is important to note that the BRF is two dimensional, with solar incidence angles that will vary and with MODIS view angles of the diffuser that are constant.

When viewing the Earth, the Earth-atmosphere bi-directional reflectance factor is given similarly by,

$$\rho_{EV,B,D}(t_{SD}) = \frac{\pi\ L_{EV,B,D}}{E_{SUN,B,D}\cos(\theta_{EV})} \tag{10}$$

Equations (9) and (10) can be combined to give

$$\rho_{EV,B,D}(t_{EV})\cos(\theta_{EV}) = \frac{L_{EV,B,D}}{L_{SD,B,D}}\rho_{SD,B,D}(t_{SD})\cos(\theta_{SD})\frac{\left[\Gamma(t_{EV})\right]^2}{\left[\Gamma(t_{SD})\right]^2} \tag{11}$$

$\Gamma(t)$ The Earth-sun distance at time t, in Astronomical Units

The ratio of the spectral radiances, $\frac{L_{EV,B,D}}{L_{SD,B,D}}$, in Equation (11) shows the use of MODIS as a ratioing radiometer with the solar diffuser as the reference sample. The ratio of the Γ terms in Equation (11) makes the reflectance product independent of the Earth-sun distance. When L_{SD} in Equation (11) is measured at a time separated from the measurement of L_{EV} (for changes in the Earth-sun distance), then L_{SD} must be corrected to correspond to the time (the Earth-sun distance) for L_{EV}.

3.1.3 Uncertainty Estimates

The fractional uncertainties in the MODIS calculated radiances and reflectances have several components. They include uncertainties in the algorithm, in the radiance and reflectance calibrations in the laboratory, and in the effects of polarization, crosstalk, and scatter within the instrument. These last three components will be scene dependent, and their magnitude is currently not known. They are not quantified in this uncertainty analysis.

Table 3.1.1 shows the current uncertainty estimates for the radiances from the MODIS solar bands. Table 3.1.2 gives the uncertainty estimates for the reflectances from these bands. The tables show the major contributors to the error budget for the laboratory calibration of the bands. The algorithm dependent terms, as given in Equations (6) and (11), are minor contributors to the error budget. These terms in the tables -- electronic non-linearity through the mirror side correction -- come from

Equation (6). For the tables, the mirror side uncertainty has been separated from the other scan angle uncertainties.

Tables 3.1.1 and 3.1.2 also include terms for short-term instrument repeatability (signal noise) and for the subsample timing of the 250- and 500-m bands. The sample times for these sub-1-km pixels are not identical. However, if these subsample times are constant, then it will be possible to flat-field these timing differences either from prelaunch calibrations or from solar diffuser measurements. The uncertainty tables include subsample timing effects as a place holder, in case the PFM data show problems.

In addition, it is important to note that, as this ATBD is published, the EOS diffuser round-robin experiment is still underway. The results from that experiment will be used to provide replacement values for the SD BRDF uncertainties in Table 3.1.2. The other uncertainties in Tables 3.1.1 and 3.1.2 will be updated, when the results of PFM testing become available. The method of reporting the uncertainties on a pixel-by-pixel basis is provided in Section 3.3.

TABLE 3.1.1 -- Radiance Calibration Uncertainties

TABLE 3.1.1 Concluded -- Radiance Calibration Uncertainties

TABLE 3.1.2 -- Reflectance Calibration Uncertainties

TABLE 3.1.2 Concluded-- Reflectance Calibration Uncertainties

3.2 The Emissive Infrared Bands

The derivation of the emissive infrared radiance equation is easier to describe when the formulation is a linear one. That is done first. A quadratic expression is more typical for the detectors so a second expression is developed. The version 2 quadratic expression is TBD. The version 2 code will use the linear expression unless analysis of the PFM data shows that one or more detectors on a band are nonlinear; in such a case the code will use to the nonlinear expression. Selection of the linear expression for emissive infrared calibration will be made on a band-by-band basis.

The procedure for producing the emissive infrared radiometric product starts with the Level 1A digital numbers (12 Bits) and involves the operations defined by equation (20) to produce the calibrated radiances. These radiances are re-interpreted as 15 bit digital numbers and are coupled with gain and offset values which are stored in the metadata to provide coded radiance values. The product is stored in integer format to save on storage volume compared to floating point storage requirements. Bit 16 (MSB) is used as a quality flag.

Each MODIS emissive infrared detector has an output consisting of a small signal superimposed on a large, variable background. The calibration process isolates the Earth view signal from the background. The calibration parameters for a linear system in the infrared are the gain and offset (background signal) and these are determined on each scan line. For a nonlinear system, the quadratic (detector) characteristics are determined from the thermal vacuum testing and are assumed to be constant. The gain and offset terms of a quadratic system still are determined on each scan line. The effective spectral emissivity and effective (spectral) temperature of the blackbody are determined also from the thermal vacuum testing.

On orbit the scan cavity and the blackbody (which floats at the scan cavity temperature) are expected to be at 259K at the beginning of life, at 269K at the middle of life, and at 279K at the mission end of life. The blackbody can be heated to 315K on orbit. Consequently, the quadratic terms for the nonlinear system can be verifies on orbit for the scene temperature ranges between the operating blackbody temperature at 315K. The thermistors for the blackbody saturate at temperatures below about 274K. Consequently the normal operating configuration of the on-board blackbody is expected to be heated for most of the mission so that we can obtain an on-scale temperature reading for the blackbody effective temperature.

3.2.1 Basic Linear Measurement Equations

The total radiance on a detector is a composite of signal through the earth view port and total signal from the instrument scan mirror and optical background. The voltage response of a detector to this composite signal is expressed in general terms as:

$$V_s = V_{scene} + V_{mirror} + V_{background} + V_{offset} \qquad (12)$$

where

V_s Analog signal voltage from Focal Plane (FPA) when the scan mirror is viewing bb, sv, ev.
s an index, indicating emissive sources: bb, sv, ev,
V_{offset} accounts for any voltage offset in the detector for zero signal

The MODIS emissive infrared band response is expected to be predominately linear, therefore, the baseline equation retrieving the band-averaged Earth view radiance, L_{ev}, is derived through the following basic linear equation relating the detector voltage response to the radiance as

$$V_{s,AOI} = m\int_0^\infty \rho_{AOI,\lambda} L_{s,AOI,\lambda} R_\lambda^{opt} d\lambda + \int_0^\infty \left(1-\rho_{AOI,\lambda}\right) B_{mir,\lambda} R_\lambda^{opt} d\lambda + L_{bkg} + V_0 \qquad (13)$$

where

m Linear calibration coefficient or system gain.

V_0 Zero flux output voltage from the detector.

$\rho_{AOI,\lambda}$ On-orbit scan mirror spectral reflectivity (and is a function of angle of incidence).

$L_{s,AOI,\lambda}$ Spectral radiance on the scan mirror when the scan mirror is viewing the source *s*.

R_λ^{opt} Optical Relative Spectral Response (RSR), which, after being multiplied by the scan mirror reflectivity $\rho_{s,\lambda}$, gives the system RSR, R_λ

$B_{mir,\lambda}$ Planck spectral radiance evaluated at the scan mirror temperature, and the associated term $\left(1-\rho_{AOI,\lambda}\right)B_{mir,\lambda}$ accounts for the scan mirror thermal emission.

L_{bkg} Optical background radiance.

After some re-arrangement of the terms in Eq.13, the basic linear equation becomes

$$V_{s,AOI} = m\Delta L_{s,AOI,\lambda} + V_0' \qquad (14)$$

where

$$\Delta L_{s,AOI,\lambda} = \int_0^\infty \rho_{AOI,\lambda}\left(L_{s,AOI,\lambda} - B_{mir,\lambda}\right)R_\lambda^{opt} d\lambda \quad , \qquad (15)$$

and

$$V_0' = V_0 + m\left(\int_0^\infty B_{mir,\lambda} R_\lambda^{opt} d\lambda + L_{bkg}\right) \qquad (16)$$

The temperature of the scan mirror is measured on-orbit and the spectral response versus scan angle of the mirror was determined prelaunch based on models and witness sample measurements. V_0' in equation (16) is the collection of terms which are constant over mirror angle of incidence, for all frames, on each scan line. The detector offset, V_0, will change slowly and may be influenced by 1/f noise. In the MODIS design, we get a scan-by-scan gain in less than 1.5 sec with about 120 μsec between blackbody and space view data collection. Consequently in the present algorithm, we will not include a 1/f correction. Analysis of the PFM thermal vacuum data set will be used to validate this assumption. Instrument background radiance, L_{bkg}, is sampled every scan also with the space view. Mirror temperature is available on-orbit to complete the evaluation of V_0'. $\Delta L_{s,AOI,\lambda}$ in equation (14) is the mathematical collection of terms which vary across the scan.

Next we use a scan line-by-scan line measurement of the on-board blackbody and the space view, for equation (14), it is determined that

$$m = \frac{V_{bb} - V_{sv}}{\Delta L_{bb} - \Delta L_{sv}}, \qquad (17)$$

$$V_0' = \frac{V_{sv}\Delta L_{bb} - V_{bb}\Delta L_{sv}}{\Delta L_{bb} - \Delta L_{sv}} . \quad (18)$$

For equations (17) and (18), knowing the temperature of the on-board blackbody and the scan mirror, we can compute ΔL_{bb} and ΔL_{sv} using equation (15). V_{bb} and V_{sv} are values measured on each scan line. This process is accomplished each swath for each band. Processing is done separately for each mirror side.

Next we want to examine equations (15) and (16) to obtain the expression for the scene radiance expressed in terms of the detector (voltage) response. Solve equation (15) for $\Delta L_{s,\,AOI,\lambda}$ and insert this expression into equation (16);

$$\int_0^\infty \rho_{AOI,\lambda} L_{ev,AOI,\lambda} R_\lambda^{opt} d\lambda - \int_0^\infty \rho_{AOI,\lambda} B_{mir,\lambda} R_\lambda^{opt} d\lambda = \frac{V_{EV,AOI} - V_0}{m} \quad (19)$$

Dividing both sides of this equation by $\int_0^\infty R_\lambda d\lambda$ permits (19) to be written in the form

$$L_{EV,B} = B_{mir,\lambda} + \frac{V_{EV,AOI} - V_{0,B}}{m\int_0^\infty R_\lambda d\lambda} \quad (20)$$

where the reported radiance product is a band average product and where

$$L_{EV.B} = \frac{\int_0^\infty L_{EV.B} R_\lambda d\lambda}{\int_0^\infty R_\lambda d\lambda} , \quad (21)$$

$$B_{mir} = \frac{\int_0^\infty B_{mir,\lambda} R_\lambda d\lambda}{\int_0^\infty R_\lambda d\lambda} \quad (22)$$

and $R_\lambda = \rho_{AOI,\lambda} R_\lambda^{opt}$.

Equation (20) must be evaluated on a pixel-by-pixel and frame-by-frame basis (for each angle of incidence on the scan mirror). The R_λ^{opt} is evaluated for channel (detector 5) in each band.

Differences in system response for channels within a band will be normalized (flat fielded) to minimize the spectral radiance differences in a band by observation of the on-board blackbody. This could be done on a scan-by-scan basis, but the current design provides this as an input parameter determined off-line.

3.2.1.1 The Master Curve Premise and Quadratic Calibration Equation

The MODIS emissive infrared band detector response is expected to be predominately linear. More generally it can be described as a quadratic function of the detector total incident radiant flux [T. Pagano, 1993; I.L.Goldberg, 1995] as

$$V_s = a\left(\Phi_s + P_x\right)^2 + b\left(\Phi_s + P_x\right) + V_0 \qquad (23)$$

where Φ_s represents the radiance on the detector from an emissive scene, *a* and *b* are the quadratic and linear calibration coefficients, and P_x represents the instrument background radiant flux. This is the MODIS calibration master curve (Figure 6) proposed by SBRS to be applicable to both the PV and PC detector bands. Bands 20 through 30 are HgCdTe photovoltaic bands and are considered likely to be linear. Bands 31-36 are HgCdTe photoconductive bands and are considered less likely to be linear.

The MODIS instrument incorporates hardware and on-board software features to continuously apply a DC restore voltage to the PV and PC preamplifiers. Its purpose is to maintain the dynamic range from the earth scene within the specified limits as the instrument background changes due to instrument temperature changes (N.B., the FPA temperatures are considered separately). As the background flux changes the calibration curve (equation) characterizing the instrument response is considered to be constant. This is shown in Figure 6, where the location of the dynamic range along the master curve shifts with P_x, for a constant calibration curve.

The DC restore voltage is available from the telemetry; therefore, Eq.23 can be directly applied. The MODIS differs from the traditional formulation used for some heritage instruments where the derived flux (or radiance) is a quadratic function of the output voltage. For heritage sensors DC restore has not been available in the telemetry stream.

The calibration curve will vary as the FPA temperature changes. However, the MODIS has been designed to maintain a "closed loop" temperature control of the SWIR/MWIR FPA and the LWIR FPA within narrow temperature control limits (83±0.005K, 85±0.005K and 88±0.005K). Two FPA temperature conditions will be tested prelaunch to characterize the calibration curve as a function of the FPA temperature. In addition to this closed loop mode, both of the focal planes, located on the common cold stem of the radiation cooler, can be operated “open loop” by commanding the temperature control heaters off. This feature is accommodated by setting an additional testing point at the open loop temperature in thermal vacuum. Colder FPA temperatures enhance detector responsivity.

The thermal vacuum test progress was constructed on the basis of the validity of this master curve concept.

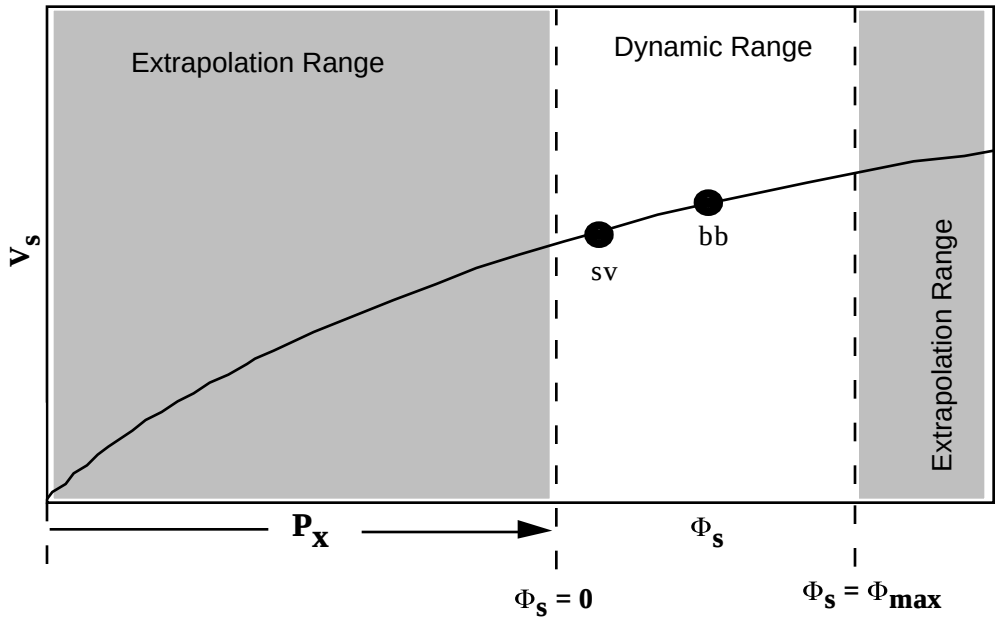

Figure 6: ***The emissive band calibration master curve***

Based on the master curve Eq.23, the following system level at-aperture radiance equation can be derived [Knowles, 1996],

$$V_s = \alpha m^2 \left(\Delta L_s + L_0\right)^2 + m\left(\Delta L_s + L_0\right) \tag{24}$$

where

α Pre-launch measured system nonlinearity ($\alpha = a/b^2$ with respect to Eq.23).
m Linear calibration coefficient or system gain.
ΔL_s As defined in Eq.26.
L_0 Background irradiance and bias.

Note that as the system nonlinearity α goes to zero, Eq.23 becomes identical to the linear equation of Eq.14, except that V_0 in Eq.13 has been absorbed in L_0. There are three calibration parameters, α, m and L_0, captured in Eq.24. The non-linearity α will be measured prelaunch at four FPA temperature conditions mentioned above, and will be interpolated on-orbit based on the FPA temperature. The other two parameters will be determined every scan by using the BB and SV measurements as

$$m = \frac{\sqrt{1 + 4\alpha V_{bb}} - \sqrt{1 + 4\alpha V_{sv}}}{2\alpha\left(\Delta L_{bb} - \Delta L_{sv}\right)}, \tag{25}$$

$$L_0 = \frac{-1 + \sqrt{1 + 4\alpha V_{sv}}}{2\alpha m} - \Delta L_{sv} \tag{26}$$

and probably, pending analysis of PFM thermal vacuum testing data, a few scans will be used to obtain an averaged and therefore relatively constant m and L_0 over many scans.

The final L1B band-averaged Earth scene radiance product is

$$L_{ev} = B_{mir} + \frac{-1 + \sqrt{1 + 4\alpha V_{ev}} - 2\alpha m L_0}{2\alpha m \int R_\lambda d\lambda} \ , \qquad (27)$$

which is applied on a per pixel basis. Indices describing the appropriate level of detail (pixel, frame, scan number and mirror sides) are suppressed at this summary level. Note that as α goes to zero, Eqs. 25-27 collapse to the corresponding linear equations 17, 18, and 20, by observing the expansion of the square root to the first order of α, $\sqrt{1 + 4\alpha x} \quad 1 + 2\alpha x$, and linear equation offset $V_0' = mL_0$.

The linear calibration equations will be used as the Level 1B emissive infrared band baseline calibration equations band by band. In the instance where we cannot achieve the required accuracy with a linear formulation for a band based on the thermal vacuum data, a quadratic calibration equation will be implemented. The details of the implementation of Eq. 23 is TBD.

3.2.1.2 *Conversion from MODIS Counts to Detector Preamplifier Output Voltage*

The analog detector output is converted to digital counts by an Analog to Digital Converter (ADC). Each of the ADCs is mapped by determining the digital output (12 bit) in response to precisely controlled voltage increments from a 16 bit voltage supply source. This mapping will be represented as prelaunch LUTs, incorporating the ADC nonlinearity effects. A combined LUT representing these results is $V_{ADC}\{DN\}$, denoting the input voltage to an ADC with the given output DN.

The A/D converters for the PV bands (ACE) are identical in design to those used for the reflected solar bands. There are two ACEs for the PV bands, one for bands 20-26 and another for bands 27-30. The PC bands have individual ACEs. The ACE for each PC band has fewer channels to digitize, so they can operate at slower speeds and are more linear than those used in the PV bands.

For the PV bands, the digital counts to voltage transfer equation is

$$V_s^{PV} = \frac{V_{ADC}\{DN_s\}}{G_1 G_2 G_3 G_4} - V_{DC}^{PV}, \qquad (28)$$

where four gain factors and one DC restore voltage value (continuously adjusted by an on-board software algorithm and reported by telemetry) are applied. G_1, G_2 and G_4 are fixed hardware values, and G_3 can be changed by command uploads to periodically restore the output dynamic range to specified values. G_3 also appears in the telemetry.

For the PC bands, the digital counts to voltage transfer equation is

$$V_s^{PC} = \frac{V_{A/D}\{DN_s\}}{G_1 G_2} - V_{DC}^{PC}, \qquad (29)$$

where

$V_{DC}^{PC} = \frac{V_{DC2}}{G_1} + V_{DC1}$, and two fixed gain factors and DC restore voltages are applied.

Errors in our knowledge of either the gain or the DC restore with not impact the uncertainty of the radiance product from Eq 20 so long as the gain and DC restore do not change over the period that the slope m is computed, i.e., usually a single scan line.

3.2.1.3 *The Calibration Transfer*

MODIS uses an aluminum v-groove blackbody mounted inside the scan cavity as its emissive infrared band on-board calibrator. The radiometric calibration transfer to the BB is accomplished by determining the effective BB emissivity and temperature using the prelaunch BCS standard. The basic calibration transfer equation can be expressed as

$$\min\left|L_{BCS}^{source}\left(B_1, \varepsilon_{BCS}^{model}, T_{BCS}^{meas}\right) - L_{BCS}^{L1B}\left(B_1, \varepsilon_{B_1}^{BB\_nom} + \Delta\varepsilon_{B_1}^{bb}, T_{bb} + \Delta T_{Band\_i}^{bb}\right)\right| \qquad (30)$$

The optimization is accomplished on a band-by-band basis. The label bb is used as reference for parameters of on-board blackbody. Strategies to accomplish this optimization are reviewed in Table 3.2.1.3.

Table 3.2.1.3: BCS to MODIS - Infrared Calibration Transfer Candidate Methods

Goal: Minimize $\left| L_{BCS}^{source}\left(B_1, \varepsilon_{BCS}^{model}, T_{BCS}^{meas}\right) - L_{BCS}^{L1B}\left(B_1, \varepsilon_{B_1}^{BB\_nom} + \Delta\varepsilon_{B_1}^{bb}, T_{bb} + \Delta T_{Band\_i}^{bb}\right)\right|$

Method	Description	Comments
1	· Select nominal emissivity values, $\varepsilon_{B_1}^{bb\_nom}$ for each band using OBC BB model and BB coupon emissivity measurements. $\left[\Delta\varepsilon_{B_1}^{bb} = 0\right]$. · Vary $\Delta T_{Band\_i}^{bb}$ to achieve best fit and apply this correction term as a constant pending updates from vicarious calibrations.	· Errors in $\varepsilon_{B_1}^{bb\_nom}$ are absorbed in $\Delta T_{Band\_i}^{bb}$ · $\Delta T_{Band\_i}^{bb}$ are not physically meaningful in terms of difference between bulk temperature and skin temperature, but perhaps capture the effective BB temperature considering all contributing sources.
2	· Use OBC measured bulk temperature, T_{bb} (average of 12 thermistors during calibration collect). $\left[\Delta T_{Band\_i}^{bb} = 0\right]$. · Vary $\Delta\varepsilon_{B_1}^{bb}$ to achieve best fit and apply this correction term as a constant pending updates from vicarious calibrations.	· Errors in the OBC BB bulk temperature, T_{bb}, are absorbed in $\Delta\varepsilon_{B_1}^{bb}$ · $\Delta\varepsilon_{B_1}^{bb}$ are not physically meaningful in terms of actual emissivity values, but perhaps capture the effective BB emissivity considering all contributing sources.
3	· Determine a constant value for $\Delta T_{Band\_i}^{bb}$ for all bands by applying the nominal emissivity, $\varepsilon_{B_1}^{bb\_nom}$ to the above transfer equation for only the bands near the peak of the Planck curve (e.g., Bands 39-31). · Applying the constant, ΔT^{bb}, determine the required $\Delta\varepsilon_{B_1}^{bb}$ values to achieve calibration transfer.	· Tends to solve for the best physical value of the difference between the BB bulk temperature and effective skin temperature using the highest SNR and most temperature sensitive bands. · $\Delta\varepsilon_{B_1}^{bb}$ are not physically meaningful in terms of actual emissivity values, but perhaps capture the effective BB emissivity considering all contributing sources.
4	· Simultaneously vary both $\Delta\varepsilon_{B_1}^{bb}$ and $\Delta T_{Band\_i}^{bb}$ for each band to achieve best fit and apply these correction terms as constants pending updates from vicarious calibrations	· Provides more degrees of freedom to satisfy the transfer equation across all bands and for all BCS radiance levels. · May be several solutions (pairs of $\Delta\varepsilon_{B_1}^{bb}$ and $\Delta T_{Band\_i}^{bb}$) to the transfer equation.

3.2.1.4 *Summary of the Calibration Parameters*

For the purpose of simplicity, the detail levels of indices are suppressed when the top level of the calibration equations were presented in the previous sections. In this section, a summary of the calibration parameters and their associated indices and properties are discussed in Table 3.2.1.4.

Table 3.2.1.4. Summary of Calibration Parameters, Types and Indices

Parameter Description	Parameter Notation	Type	Index
Relative Spectral Resp.	R_λ	1	B
Scan Mirror Refl. @ bb, sv	$\rho_{s,\lambda}$ (s=bb,sv)	1	B,MS
Scan Mirror Refl. @ ev	$\rho_{ev,\lambda}$	1	B,MS,F
OBC BB emissivity& offset	ε_{bb}, $\Delta\varepsilon_{bb}$	1	B
OBC BB temp correction	ΔT_{bb}	1	B
System gain or linear coef	m	3	D,S
Background radiance	L_0	3	D,S
System RVS @ EV sector	D_{ev}	4	B,MS
FPA voltage @EV,BB,SV	V_s (s=ev,bb,sv)	3	D,F
Thermistor reading of Temp	T_s (s=mir,bb)	5	S
DN values @ EV,BB,SV	DN_s (s=ev,bb,sv)	5	D,F

where, D=Detector, B=Band, MS=Mirror Side, F=Frame, S=Scan, and
Type 1: Pre-launch measured or model-estimated variables, represented as Look-Up-Table (LUT).
Type 2: Pre-launch measured and post-launch interpolated (or extrapolated) variables.
Type 3: On-line scan-by-scan measured variables.
Type 4: Off-line measured variables via S/C maneuver observing space through Earth aperture; the data are based on witness sample measurements of the scan mirror until the deep space maneuver is accomplished.
Type 5: Telemetry data.

3.2.2 Uncertainty Analysis

The radiometric uncertainty of the MODIS emissive infrared band calibration is derived in a formal way as a small perturbation about nominal values and is summarized as

$$\left(\frac{\Delta L}{L}\right)_{total} = \sqrt{\underbrace{\left(\frac{\Delta L}{L}\right)^2_{algorithm}}_{\substack{algorithm-based\\ estimate}} + \underbrace{\left(\frac{\Delta L}{L}\right)^2_{NIST-BCS}}_{\substack{NIST-BCS\\ radiance-transfer}} + \underbrace{\left(\frac{\Delta L}{L}\right)^2_{Crosstalk} + \left(\frac{\Delta L}{L}\right)^2_{Scatter}}_{\substack{Scene-dependent\\ (not-included-in-V\,2.0-L1B)}}} \qquad (31)$$

The algorithm-based term is the sum of the individual contributions of the L1B emissive infrared calibration parameters to the EV radiance calculations; see Table 3.2.1.4. The final uncertainty product will be converted to a dimensionless index value (2^4 gray levels). This arrangement is to provide an efficient as well as space-saving algorithm to calculate the L1B radiance uncertainty product on a pixel-by-pixel basis.

A model of MODIS output was generated using a center wavelength based analysis and an estimation of the radiometric uncertainty for each band was then determined for typical scene

radiance. Tables 3.2.2 and 3.2.3 show a summary of these results for each of the MODIS emissive infrared PV and PC band, respectively. Some of the parameters, w_{cav}, w_{sv}, T_{sam} and T_{swath}, are not listed in Table 3.2.1.4, because they are associated with stray-light problems, and the magnitude of their contribution needs further investigation. They will be discussed in Section 3.2.3.1.

Table 3.2.2 Typical Radiance Uncertainty Contributions and RSS Total for PV Bands

Table 3.2.3 Typical Radiance Uncertainty Contributions and RSS Total for PC Bands

3.2.3 Constraints, Limitations and Assumptions

The emissive infrared band calibration algorithm assumes an almost perfect instrument without addressing any detector noise (1/f noise in particular) and instrument spurious effects. The MODIS instrument likely will not behave in such ideal way, and the L1B emissive algorithm will have to include many correction terms in order to meet the specification of the emissive infrared band calibration accuracy. The algorithm described above represents the relatively well understood "clean" part of the MODIS instrument. Detector noise and instrument spurious effects still need further investigation. In addition model validation must be done; the strategy for doing this is to make use of the prelaunch thermal vacuum test data and post-launch data.

In this section, instrument spurious source corrections will be discussed based on current understanding of the problems.

3.2.3.1 *Instrument Spurious Source Corrections*

In general, each of the measured at-aperture radiances, represented by Eq.23 with ev replaced with sv and bb, will be contaminated by radiation from sources other than the nominal "within-the-Field-of-view" scene radiance. These spurious contamination sources, to the extent that they are determined to be significant by characterization or modeling, can be accounted for by making the following identifications:

$$L'_{ev} \rightarrow L_{ev} + L^{ev}_{emiss}(T_{cav}) + L^{ev}_{scene\_refl}(T_{scene}) \quad (32)$$

$$L'_{sv} \rightarrow L_{sv} + L^{sv}_{emiss}(T_{cav}) + L^{sv}_{scene\_refl}(T_{scene}) \quad (33)$$

$$L'_{bb} \rightarrow L_{bb} + L^{bb}_{emiss}(T_{cav}) + L^{bb}_{scene\_refl}(T_{scene}) \quad (34)$$

where the first terms on the right-hand-side designate the nominal radiance as seen by EV, SV, and BB respectively, L_{emiss} and L_{scene_refl} represent the radiance from cavity emission sources and scene radiance sources scattered or reflected into the MODIS FOV, and T_{cav} and T_{scene} represent the scan cavity and scene temperatures, respectively.

During the spacecraft maneuver to view deep space through the Earth aperture, the Earth scene spurious radiance source terms will be zero, enabling measurement of the cavity emission spurious source terms. To the extent that cavity temperature dependent contamination source terms are measurable as a result of the deep space view maneuver, corrections terms can be incorporated into the algorithm. Unique measurement of the scene temperature dependent terms is more difficult. This will require careful assessment of instrument performance in response to specific scene contrast features.

Preliminary analyses indicate that the effects of some of these spurious terms are negligible; others are still to be determined (using PFM test data) and therefore not included in the current correction algorithm. The current correction algorithm uses a simpler version of Eqs. 32-34,

$$L'_{ev} \rightarrow L_{ev}\,, \quad (35)$$

$$L'_{sv} \rightarrow L_{sv} + L^{sv}_{emiss}(T_{cav})\,, \quad (36)$$

$$L'_{bb} \rightarrow L_{bb} + L^{bb}_{emiss}(T_{cav}) + L^{bb}_{scene\_refl}(T_{scene}) \quad (37)$$

The correction term identified for the space view (Eq.36) is incorporated as a weighting factor applied to the Planck function for the space view surround temperature, characterized by the temperature of the Space Analog Module (SAM) electronics, T_{SAM}

$$L'_{sv} \rightarrow L_{sv} + w_{sam} L_{cav}(T_{SAM}) \quad (38)$$

where w_{sam} is determined initially from modeling estimates.

The correction terms identified for the BB are incorporated as weighting factors applied to the Planck function for the cavity and scene temperature, respectively,

$$L'_{bb} \rightarrow L_{bb} + w_{cav} L_{cav}(T_{cav}) + w_{scene} L_{scene}(T_{scene}) \quad (39)$$

where w_{cav} and w_{scene} are determined initially from modeling estimates. This formulation treats the blackbody reflection of scene radiance into the MODIS FOV as an effective diffuse process, thus enabling a simpler correction process.

3.3 Practical Considerations

The Level 1B processing in the routine production environment requires access to three contiguous Level 1A files in order to correctly handle averaging, statistics and calibration at the beginning and end of the file being calibrated. The production rules specify this requirement for execution at DAAC.

The L1B reflective band calibration data flow diagram is :

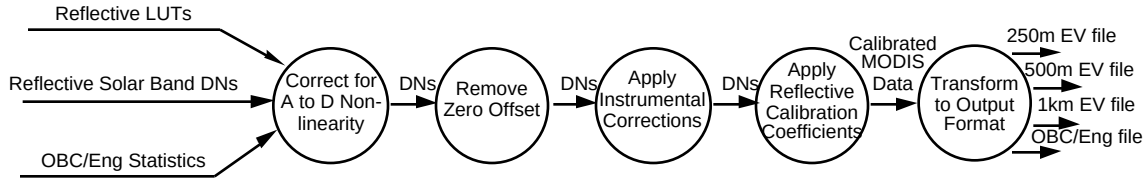

The L1B emissive band calibration data flow diagram is:

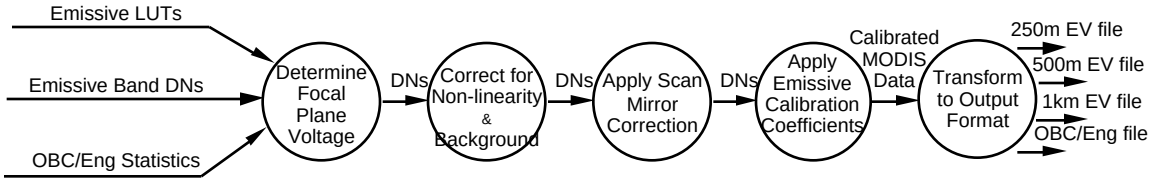

3.3.1 Programming Considerations

The software implementation of the algorithm takes into consideration efficient use of computing resources and ease of maintenance in the production environment. The software system makes extensive use of look-up tables generated in the CROM instead of direct computations in the

production system. This technique reduces CPU requirements in the production environment by moving computation of stable or slowly varying terms out of the time-critical production stream. This technique also minimizes changes to the production code in the instances where MCST is uncertain about either the instrument effect or the method to compute the calibration equation and parameters to describe the effect. Changes to instrument characteristics or to the way these characteristics are determined are provided as updated input datasets rather than new versions or releases of the production software. These tables are sized to include expected parameter ranges with a resolution determined to minimize both interpolation errors and software memory use.

3.3.2 Quality Control and Diagnostics

The Level 1B production software monitors and reports many conditions which may effect the calibration coefficients, and therefore the calibration of the data. The reporting function is carried out using a combination of data flags and messages written to the Level 1B processing log.

Invalid data fields are identified within the Level 1B product. The data in a field is marked as invalid for the following reasons:

it was flagged as missing from the Level 1A dataset;
the detector is dead;
the value was saturated;
there was a calibration failure;
the radiance was too low to calculate;
there was coherent Space View (SV) noise;
the number of outliers in the SV data exceeded the maximum;
there was a mirror side difference in the SV data.

Granule level metadata contains information about the quality of the data within the granule. Four searchable fields store indicators of routine or non-routine instrument operations; good, marginal or bad calibration data quality; nadir or non-nadir pointing attitude; and Activation and Evaluation (A&E) or post A&E mission phase. Non-searchable fields describe

Number of Scans
Number of Day mode scans
Number of Night mode scans
Incomplete Scans
Max Earth View Frames
%Valid EV Observations
%Saturated EV Observations
Post Processing Indicates Bad data
Electronics Redundancy Vector
Reflective LUT Last Change Date
Emissive LUT Last Change Date
Focal Plane Set Point State

In addition, each scan has a set of flags to indicate

Moon in SV Port
Spacecraft Maneuver
Sector Rotation
Negative Radiance
Beyond Noise Level

PC Ecal on
PV Ecal on
SD Door Open
SD Screen Down
SRCA On
SDSM On
Outgassing
Instrument Standby Mode
Linear Emissive Calibration
DC Restore Change
BB/Cavity Temperature
Differential
BB Heater On
Missing Previous Granule
Missing Subsequent Granule

Messages describing these conditions are written to the message logs using the Status Messaging Facility (SMF) supported in the Science Data Processing Tool Kit (SDPTK). The Level 1B Product Specification contains a detailed description of these fields.

3.3.3 Exception Handling

Exception handling in the Level 1B production software is designed for reliable data processing. The volume of data and the time constraint on availability of the output for downstream processing makes it essential that exceptions are handled in such a way that processing may continue if at all possible. Only catastrophic failures will terminate execution. All other exceptions are handled by flagging, and reported in the processing log. MCST will monitor the types and frequency of exceptions that occur during routine Level 1B data production. This information will be used to improve the calibration algorithm and the software.

The averaging algorithm used for SV data, BB data and thermistor data uses a predetermined number of scans in a moving window. If there is data drop out, or if the Level 1A files which precede or are subsequent to the file to be calibrated are not available for processing, the prescribed number of scans for averaging will not be available near these data edges. This algorithm handles edges of data by starting with the first available scan and increasing the number of scans used in the average until the specified number of scans can be used. The uncertainty index is increased for each scan that was calibrated using averages calculated from fewer than the required number of scans in the window.

Handling of the averaging algorithm and the calibration when DC Restore takes place, when DC Restore occurs when the moon is visible in the SV port, and when DC Restore is commanded off so that the SV measurements are allowed to drift and reduce the dynamic range, is TBD.

Data acquired during non-routine instrument operations, spacecraft maneuvers, and other non-standard operating scenarios will be analyzed by MCST in the CROM facility. The methodology and results of these analyses will be made available to the user community by way of the internet and the World Wide Web.

3.3.4 Output Product

The instrument measurements stored in the output product are in the form of an integer, N, along with three pairs of scale and offset values which may be applied to the value of N to obtain the radiance, the reflectance product, and the corrected raw counts (DN*). The basis for calculating

the scale and offset values is the instrument specification for each band. This basis will not change over the life of the mission, so that the mapping of the integer, N, to the reflectance product and the radiance product for the emissive infrared bands is unique throughout the mission.

The reflectance product is relevant only to the solar reflected bands data sets. The scale and offset values are contained in the metadata. Trending analysis on the scale and offset values to convert N to DN* will allow the user to know when the system calibration parameters have been changed, except that scale factor must be adjusted for changes in the Earth-sun distance.

For each of the 330 detectors in the solar reflective bands 1-19, and 26, the L1B calibration product consists of the Earth scene spectral radiance, along with its associated uncertainty index, and a reflectance product which is the Earth scene BRF multiplied by the cosine of the scene zenith angle. The Level 1B emissive band product consists of the apparent Earth scene spectral radiance for each scene radiance, along with its associated uncertainty index. Negative radiance values attributed to noise suppression and space view surround radiance can occur. These negative values are useful for subsequent analysis and will be carried and not converted to zero.

Emissive calibration is either linear or non-linear on a per-band basis. The calibration is linear unless pre-launch testing has demonstrated that at least one detector in a band responds non-linearly. If any detector in a band behaves non-linearly during testing, all detectors in the band are calibrated using the non-linear form of the equation.

A conversion table which can be used to transform the emissive radiometric product to an effective scene temperature will be available as a separate product from the GSFC DAAC.

The radiance uncertainty index for each pixel is a 4 bit index and is defined in terms of a multiplier applied to the instrument specifications. The uncertainty is recorded as an index which includes MCST's complete and best understanding of the flat-field uncertainties for that pixel. The index translates to an uncertainty value by use of the formula

exp(Uncertainty Index/2) = $\pm$Uncertainty Range Multiplier Value.

Specifically,

(ΔL/L) = (Accuracy requirement for the band) * (Uncertainty Range Multiplier)

The uncertainty is carried in the one-sigma sense. This index can be considered a Risk Index describing the use of the Level 1B data. An Uncertainty Index of 7 indicates that the uncertainty has not been computed.

An additional index of 4 bits is reserved for each pixel for a scene contrast uncertainty. The details of this index are TBD. The output product is defined in greater detail in the MODIS Level 1B Product Specification and the MODIS Level 1B Product User's Guide.

4. OFF-LINE ANALYSIS CONTRIBUTION, VICARIOUS CALIBRATION, MONITORING/TRENDING, AND CONSTRAINTS

T/V TEST ANALYSES

Thermal Vacuum testing is the closest the instrument gets to being in the environment it will see on orbit. As such, it is the only time that the radiative cooler and thermal bands operate as we expect in normal operations. SBRS ran multiple tests during T/V to characterize the instrument in its "operational state" and collect parameters that are impossible to collect once the instrument is

launched (like non-linearity, LWIR spectral shape, etc.). In addition, these tests are used to demonstrate specification compliance.

MCST uses the data from Thermal Vacuum in two ways. First, the instrument data are used as test data sets for the algorithm. Second, many of the parameters required by the Level 1B code are calculated using these test data sets.

Particular studies that will be performed on the thermal vacuum data sets include assessing the need to use a non-linear algorithm for the PC emissive infrared bands, assessing the sensitivity of the SWIR bands (HgCdTe detectors) to sensor thermal background, temperature sensitivity for the electronics and non-uniform sampling of Bands 1-7 (the sub 1-km bands). Other studies with the thermal vacuum include assessment of 1/f noise within the context of our ATBD equations and the adequacy of a single RSR per band in comparison to a unique RSR per detector. The assumptions in section 3.2.3.1 on instrument spurious scattering will be validated. No crosstalk errors or correction algorithms are included in the ATBD Version 2.0; that principle will be validated with thermal vacuum data.

Uncertainties due to water vapor and other atmospheric constitutes must be investigated in the spectral and radiometeric data.

4.1 Vicarious Calibration

An Overview

MODIS has a set of challenging requirements for radiometry and for other measurements (see Appendix C). These requirements are imposed by the science needs of the Level 2 products derived from MODIS. In order to assure these science needs are met it is beneficial to have available several independent methods to establish and verify important components of the instrument calibration throughout the mission. Vicarious calibration (VC) that provides the critical independent determinations of radiance or reflectance at the MODIS aperture for a given detector at a specific time. Combining ground/aircraft radiance measurements with the instrument response in counts provides the independent responsivity determinations needed to verify or modify the MODIS calibration.

Vicarious methods are reliable because they exercise the operational imaging mode of the sensor and implicitly account for size of source effects. However such calibrations are made much less frequently than on-orbit calibrations and usually yield much fewer data points (order of magnitude of 10 TOA radiances per field campaign).

The SRCA is crucial to many on-orbit characterization studies for MODIS, and these are described in a specific SRCA section at the end of Section 4.

4.1.1 Vicarious Calibration and the MCST Strategy

The application of vicarious calibration measurements to the MODIS reflective band calibration algorithm is accomplished via the multiplicative correction factors, $F_{VC,L,B,D}$ (Eq 5) and $F_{VC,\rho,B,D}$ (Eq 8). In the thermal bands the information from vicarious calibration will be used to change temperature offsets of the average BB and cavity temperatures. Vicarious calibrations are expected to be most useful for checking overall radiometric scales. Tables 4.1 and 4.2 describe the primary utility for vicarious calibrations for spectral, spatial, and radiometric calibration and

characterizations. These tables are preliminary, and will be expanded with more measurements and supporting detail in a Validation Plan.

Table 4.1
Vicarious Calibration Matrix
Reflected Solar Bands

Band	Spectral	Spatial		Radiometric			
				Radiance		Reflectance	
	Center Wavelength	Geo-location	Co-registration	Uncertainty	With-in Orbit Stability	Uncertainty	With-in Orbit Stability
1	B	D	F	G,H,I,L	J	O	N
2	B	D	F	G,H,I,L	J	O	N
3	A	D	F	G,L	J	O	N
4	A	D	F	G,H,I,L	J	O	N
5	C	E	F	L	J	O	N
6	C	E	F	L	J	O	N
7	C	E	F	L	J	O	N
8	A	D	F	L	J	O	N
9	A	D	F	L	J	M,O	N
10	A	D	F	G,H,I,L	J	O	N
11	B	D	F	G,H,I,L	J	O	N
12	B	D	F	G,H,I,L	J	M,O	N
13	B	D	F	H,I,L	J	M,O	N
14	B	D	F	H,I,L	J	O	N
15	B	D	F	H,I,L	J	O	N
16	B	D	F	H,I,L	J	M,O	N
17	B	D	F	H,I,L	J	O	N
18	B	D	F	H,I,L	J	O	N
19	B	D	F	G,H,I,L	J	O	N
26	C	E	F	L	J	O	N

A: SRCA Spectral Mode, center wavelength uncertainty less than 0.5 nm
B: SRCA Spectral Mode, center wavelength uncertainty between 0.7 and 0.8 nm
C: SRCA Spectral Mode, center wavelength uncertainty between 0.5 and 1.0 nm
D: Geolocation navigation with single band from VIS, NIR focal planes. Reference geolocation can be validated for other bands on VIS, NIR focal planes, and through co-registration from SRCA spatial
E: Geolocation using co-registration between geolocated band from VIS, NIR focal plane and SRCA spatial
F: All bands, all channels co-registered using SRCA spatial for scan direction, and band centroid in track direction
G: Land surface vicarious calibration methods such as performed by Slater
H: Ocean surface vicarious calibration methods such as performed by Clark
I: High altitude aircraft underflights such as performed by Abel
J: SRCA radiometric mode, 10W and 1W lamp, in continuous operation
K: Assessed with uncertainty of radiance product and comparison of irradiance measurements from SD to solar spectra irradiance standard spectra
L: SDSM tracking of SD stability
M: Comparison with MISR and OCTS radiance
N: Comparison with reflections from the moon
O: Comparison of MODIS solar spectral irradiance with published values of the same

Table 4.2
Vicarious Calibration Matrix
Emissive Infrared Bands

Band	Spectral	Spatial		Radiometric		
	Center Wavelength	Geo-location	Co-registration	Uncertainty	With-in Orbit Stability	Non-Linearity
20	A	B	D	?	E	G
21	A	B	D	?	E	G
22	A	B	D	?	E	G
23	A	B	D	?	E	G
24	A	B	D	?	E	
25	A	B	D	?	E	G
27	A	C	D	?	E	
29	A	C	D	?	E	
30	A	C	D	?	E	G
31	A	C	D	F	E	G
32	A	C	D	F	E	G
33	A	C	D	?	E	G
34	A	C	D	?	E	
35	A	C	D	?	E	
36	A	C	D	?	E	

A: No established techniques; Fourier transform interferometry systems from Wisconsin may be studied as a research activity to validate the prelaunch characterization in some bands

B: Geolocation using co-registration between geolocated bands from VIS, NIR; these bands are on the same focal plane as Band 7 for which direct validation or registration is available

C: Geolocation using co-registration between geolocated band from VIS, NIR focal plane and SRCA spatial

D: All bands, all channels co-registered using SRCA spatial for scan direction, and band centroid in track direction

E: All bands use on-board blackbody and space view on each scan line

F: Comparison with ATSR, AERI and other radiometer radiances

G: Non-linear behavior of band validated over useful radiometric range using on-board black-body in elevated temperature ranges. Category selected for all bands with a L_{typ} equal to or greater than expected temperature of scan mirror and scan cavity beginning of mission

?: To be determined

After launch, MCST will regularly convene a panel of experts, representing the Science Team, to review the instrument calibration status. This panel will include experts in both reflected band and emitted infrared band vicarious calibration techniques, experts on the characteristics and preflight calibration of the MODIS instrument, and MCST members familiar with the algorithms used in the Level 1B MODIS processing. The panel will provide recommendations to the Science Team Leader. Implementation of the changes to the algorithm and calibration parameters is the responsibility of the MCST Leader working for the Science Team Leader.

The panel will review responsivities as functions of time for all of the bands as determined by the OBCs and by vicarious data sets. Useful data sets will be those shown to possess internal consistency, that include uncertainty estimates, and are traceable to NIST or other EOS approved standards.

Before changes are introduced in the MODIS calibration and characterization parameters MODIS will test the impact of these changes on the upper level products. These changes will be checked through the use of test data sets distributed to Level 1B product users.

A&E Activities and Analyses

The instrument will be turned on a few days after nominal orbit is reached. The draft Activation and Evaluation Phase MODIS early operations activity is shown in section 2.4.2. This schedule describes the current understanding of the sensor operations for the initial 17 weeks of on-orbit operations.

This activation will provide useful data for bands 1-4 and 8-19. The radiometric calibration will initially be the prelaunch value. Regular measurements with the SD will start immediately at sensor turn on. During this phase the operation, repeatability, and stability of the MODIS OBCs and the techniques developed to use them will be verified. Data trending, comparisons, and statistical analyses will begin in this phase and will continue throughout the mission to improve instrument characterization and calibration.

Validation of ρ_{EV} in Equation (11) will be assessed in part by comparison of $E_{MODIS,B}$ from Eq. 9 with published curves of the solar spectral irradiance in these wavelength regions. Uncertainty in comparison between $E_{MODIS,B}$ and the published literature will result (in decreasing order of probability) (1) in unaccounted scattering effects in the solar diffuser port, (2) in uncertainty in the laboratory measurement of ρ_{SD}, (3) in changes in the characteristics of the SD from the preflight characterization, (4) in an error in Eq.7 to compute L_{SD}, or (5) in **an error in the published literature for the solar spectral irradiance.

Flat-fielding approaches (detector equalization within a band) using the solar diffuser for the reflective solar bands, and using the blackbody for the emissive infrared bands, will be checked with “bow-tie” effects using real scenes. Bow-tie effects are derived from the scene scanning geometry that leads to a widening of the ground instantaneous field of view at larger scan angles. Detectors from adjacent bands will overlap (with different mirror sides), looking through almost identical atmospheric paths. These overlaps will allow for validation of the detector equalization constants under differing spectral distribution of the scene radiance, allow for validation of using a single RSR for all detectors in a band, and validate the co-registration from the SRCA spatial mode observations.

When the OBC stability and performance have been verified and the approaches reviewed by the Science Team, the SD measurements will be incorporated into the degradation algorithm automatically. If improvements in sensor sensitivity to temperature variations are developed through early on-orbit operations of the SRCA, these improvements will be incorporated immediately.

The cooler door will be operated about 45 days into mission operations. The BB and SV will be used for the emissive infrared calibrations immediately, based on the BB effective emissivity determined during system prelaunch thermal vacuum testing.

Vicarious calibration measurements will be used to validate the sensor product. Coincident measurements will be compared to the data product to validate the characterization and calibration of MODIS.

For MODIS data associated with lunar vicarious measurements a slightly different process is required. The lunar data are collected through the SV port rather than the EV port. When lunar mode starts, the zero radiance level determined from the SV will be frozen and maintained for the duration of the lunar mode, during which time the DN values of the SV data will be treated like EV data. Radiance and reflectance values will be calculated, applying the standard calibration formulas with the current responsivity values in both the reflected and emissive bands with the frozen background subtraction values. Radiance and reflectance uncertainty estimates will be calculated in the same way that they are calculated for EV data. The data is processed off-line. In some instances spacecraft maneuvers are required to provide quality lunar views through the space view port.

Trending, Monitoring, and Quality Assurance

Monitoring and trending in-orbit performance serves two purposes:

* it is a quality assurance function: observing and analyzing the daily behavior of a large collection of instrument parameters to ensure that the calibration is maintained over the life of the instrument, and to keep up-to-date on the health of the instrument,
* it provides the EOSDIS archive with a historical record accessible to the entire science community.

Time series are sometimes influenced by unknown interruptive events which, in turn, create spurious observations (outliers) that are inconsistent with the rest of the series. Furthermore outliers wreak havoc in data analysis, making resultant inferences unreliable or even invalid. It is important to have procedures in place to detect and remove outliers.

Baselines regarding the health of the instrument and the health of the data will be created during A&E activities. MCST will trend and monitor these baselines throughout the mission. In particular collecting, analyzing, and interpreting all of the OBC time series data, the thermistor time series data, time series associated with spatial, spectral, and radiometric behavior, and other engineering data will be accomplished for the purpose of providing a continuous screening mechanism for the detection of anomalous behavior. Knowing the answer to the question "when did a change of this particular kind occur?" naturally leads to the question "why did it occur?"

Results of these activities and studies will be reported to the MODIS Science Team through reports, memos, and presentations.

THE SRCA

The SRCA is a partial aperture, multi-mode (radiometric, spectral, spatial) calibration instrument that provides spectral calibration and radiometric calibration of the VIS, NIR, and SWIR bands. In addition the SRCA can track the band-to-band registration of all bands and establish geometric coregistration of them along track and along scan.. In the radiometric mode, the instrument response from 0.4 μm to 2.1 μm is tracked compared to prelaunch behavior with one 1 watt and up to three 10 watt lamps.

The SRCA processing is done off-line.
The Radiometric Mode

The objectives of the SRCA radiometric mode are:
1) Track changes in radiometric characteristics within orbit.

Radiometric stability of the SRCA source sub-assembly can be assessed either using a radiance controlled method in feedback from a photodiode embedded in the miniature spherical integration that houses the SRCA lamp sources, or by operating the lamp sources in a constant current mode.

The Spectral Mode

The Spectral mode is used to characterize spectral shifts in the reflected solar reflective bands. Evidence from precursor instruments suggests that such spectral shifts can occur during insertion into orbit and during on-orbit operations. The spectral response of the MODIS system is measured prelaunch for all bands, using an external double monochromator/collimator system which fills the full MODIS aperture.

The spectral calibration is operable for VIS, NIR, and SWIR bands (1-19, 26) although it is less accurate for $\lambda > 1$ μm.

The wavelength registration of the SRCA monochromator is checked on-orbit by matching with transmission lines of a didymium glass filter within the SRCA. A complete spectral scan with the SRCA will take 70 minutes, and would be subject to error if the lamp output was not stable during this period. Consequently changes in lamp output will be tracked using a silicon photodiode housed in the central obscuration of the SRCA output telescope.

Ground testing has demonstrated that the photodiode in the output telescope is contaminated by earth scenes during the daylight portions of the orbit. Consequently, the spectral calibrations with the SRCA will be limited to the night portions of the orbit, will require special data operations of MODIS to collect reflected solar bands as they are being calibrated, and the “70 minute” operations will be broken into several sequences which fit into the about 40 minutes of eclipse data periods.

The Spatial Mode

The spatial location accuracy has two aspects: (1) the accuracy of the geolocation for a single reference band, and (2) the accuracy of the coregistration of other bands relative to the reference band. The geolocation accuracy will be improved by SDST during the A&E phase using ground control points. The process is described in ATBD MOD03.

During prelaunch activities Ground Support Equipment (GSE) measures the position along scan and along track of each MODIS detector. The SRCA also measures the apparent relative position along-scan for each detector and the centroid position along-track for each band. These data are used to spatially calibrate the SRCA against the GSE. Correction coefficients are computed which account for the partial illumination SRCA aperture.

During on-orbit activities the SRCA senses the relative position shifts in the along-scan direction for each detector and the centroid shifts in the along-track direction for each band. The misregistration is computed using on-orbit data and comparing it with the pre-launch detector position.

Details of the SRCA and the calibration algorithm are documented in [Montgomery and Che, 1996].

5. APPENDIX A: PEER REVIEW BOARD ACCEPTANCE REPORT

This page intentional left blank.

6. APPENDIX B: MODIS SPECTRAL BANDS SPECIFICATION

BAND	λ	IFOV	Bandwidth	PURPOSE (Examples)
LAND AND CLOUD BOUNDARIES/PROPERTIES BANDS				
1	645 nm	250 m	50 nm	Veg. Chlorophyll Absorption
2	858 nm	250 m	35 nm	Cloud and Veg. Land Cover Transformation
3	469 nm	500 m	20 nm	Soil, Vegetation Differences
4	555 nm	500 m	20 nm	Green Vegetation
5	1240 nm	500 m	20 nm	Leaf/Canopy Differences
6	1640 nm	500 m	24.6 nm	Snow/Cloud Differences
7	2130 nm	500 m	50 nm	Land and Cloud Properties
OCEAN COLOR BANDS				
8	412 nm	1000 m	15 nm	Chlorophyll
9	443 nm	1000 m	10 nm	Chlorophyll
10	488 nm	1000 m	10 nm	Chlorophyll
11	531 nm	1000 m	10 nm	Chlorophyll
12	551 nm	1000 m	10 nm	Sediments
13	667 nm	1000 m	10 nm	Sediments, Atmosphere
14	678 nm	1000 m	10 nm	Chlorophyll Fluorescence
15	748 nm	1000 m	10 nm	Aerosol Properties
16	869 nm	1000 m	15 nm	Aerosol/Atmospheric Properties
ATMOSPHERE/CLOUD BANDS				
17	905 nm	1000 m	30 nm	Cloud/Atmospheric Properties
18	936 nm	1000 m	10 nm	Cloud/Atmospheric Properties
19	940 nm	1000 m	50 nm	Cloud/Atmospheric Properties
THERMAL BANDS				
20	3.75 µm	1000 m	0.18 µm	Sea Surface Temperature
21	3.96 µm	1000 m	0.059 µm	Forest Finfraredes/Volcanoes
22	3.96 µm	1000 m	0.059 µm	Cloud/Surface Temperature
23	4.05 µm	1000 m	0.061 µm	Cloud/Surface Temperature
24	4.47 µm	1000 m	0.065 µm	Tropospheric Temperature/Cloud Fraction
25	4.52 µm	1000 m	0.067 mm	Tropospheric Temperature/Cloud Fraction
26	1375 nm	1000 m	30 nm	Cinfraredrus Cloud Detection
27	6.72 µm	1000 m	0.36 µm	Mid-Tropospheric Humidity
28	7.33 µm	1000 m	0.30 µm	Upper-Tropospheric Humidity
29	8.55 µm	1000 m	0.30 µm	Surface Temperature
30	9.73 µm	1000 m	0.30 µm	Total Ozone
31	11.03 µm	1000 m	0.50 µm	Cloud/Surface Temperature
THERMAL BANDS				
32	12.02 µm	1000 m	0.50 µm	Cloud Height & Surface Temperature
33	13.34 µm	1000 m	0.30 µm	Cloud Height & Fraction
34	13.64 µm	1000 m	0.30 µm	Cloud Height & Fraction
35	13.94 µm	1000 m	0.30 µm	Cloud Height & Fraction
36	14.24 µm	1000 m	0.30 µm	Cloud Height & Fraction

7. APPENDIX C: KEY MODIS REQUIREMENTS

Absolute radiometric calibration accuracy (1σ @ L_{typ}) with uniform scenes		
<3µm	±5%	
>3µm, except bands 20, 21, 31, 32	±1%	
Band 20 (3.75 µm)	±0.75%	(Goal ±0.5%)
Bands 31 (11.03µm) & 32 (12.02 µm)	±0.5%	(Goal ±0.25%)
"High" band 21 (3.96 µm)	±10%	(Agreed w/ SBRC) --Not in Spec
"High" bands 31hi, 32hi	±10%	
Reflectance (Target r at TOA)	±2%	
Stability of Radiance Ratio		
Ratio of mean band responses	±0.5% @ full scale	
(max change in two week interval)	±1% @ half scale	
Spectral Characterization Accuracy		
$\lambda \leq \lambda_0$	preflight ±0.5nm	where
$\lambda > \lambda_0$	preflight $\pm 0.5(\lambda/\lambda_0)$nm	λ_0 = 1.0µm
$\lambda < \lambda_0$	on-orbit $\pm 1.0(\lambda/\lambda_1)$nm	λ_1 = 0.412µm
Spatial Characterization		
MODIS Pointing Knowledge with reference to EOS AM-1	±30 arcseconds, 1σ (±100m at nadinfrared)	
Absolute AM-1 pointing knowledge	±30 arcseconds, 1σ (±100m at nadinfrared)	
Coregistration		
1 km —>	1 km	±0.2 km (goal ±0.1 km)
0.5 km —>	0.5 km	±0.1 km (goal ±0.05 km)
0.25 km —>	0.25 km	±0.05 km (goal ±0.025 km)
1 km —>	0.5 km	±0.2 km (goal ±0.1 km)
1 km —>	0.25 km	±0.2 km (goal ±0.1 km)
Bright Target Recovery & Associated Optical Effects		
L_{cloud} —>	L_{typ} (Reflective Bands)	Output settles to < ±0.5%
L_{max} —>	L_{typ} (Thermal Bands)	within 2 km of entering L_{typ} regime

8. APPENDIX D: ACRONYMS AND ABBREVIATIONS

A/D	Analog-to-Digital Converter
A&E	Activation and Evaluation
AM-1	Ante Meridian EOS Platform
ATBD	Algorithm Theoretical Basis Document
AU	Astronomical Unit
AVHRR	Advanced Very High Resolution Radiometer
BB	OBC Blackbody
BCS	Blackbody Calibration Source
BRDF	Bi-Dinfraredectional Reflectance Distribution Function
BRF	Bi-Dinfraredectional Reflectance Factor
CARF	Combined Aperture Response Function
CARFS	CARF along-scan
CARFT	CARF along-track
CDR	Critical Design Review
CZCS	Coastal Zone Color Scanner
DAAC	Distributed Active Archive Center
DC	Dinfraredect Current
DN	Digital Number
EM	Engineering Model
EOS	Earth Observing System
EV	Earth view
FPA	Focal Plane Assembly
GSE	Ground Support Equipment
HINFRARED S	High Resolution Infrared Spectrometer
IAC	Integration Alignment Collimator
IFOV	Instantaneous Field of View
INFRARED	Infrared
K	Kelvin
LWINFRARED	Long Wavelength Infrared
MCST	MODIS Characterization Support Team
MODIS	Moderate-Resolution Imaging Spectroradiometer
MTPE	Mission to Planet Earth
MWINFRARED	Medium Wavelength Infrared
NASA	National Aeronautics and Space Administration
NINFRARED	Near Infrared
NIST	National Institute of Standards and Technology
nm	Nanometers (10^{-9} meters)
ND	Neutral Density
NOAA	National Oceanic and Atmospheric Administration
NOSC	Naval Ocean Systems Center
OBC	On-Board Calibrator
OOB	Out-of-Band
PC	Photoconductive
PM-1	Post Meridian EOS Platform
PV	Photovoltaic
RSS	Root-Sum-Square
SAM	Space Analog Module

SBRS	Santa Barbara Remote Sensing
SD	Solar Diffuser
SDSM	Solar Diffuser Stability Monitor
SDST	Science Data Support Team
SeaWiFS	Sea Viewing Wide Field of View Sensor
SiPD	Silicon Photodiode
SIS	Spherical Integrating Source
SNR	Signal-to-Noise Ratio
SPMA	Spectral Measurement Assembly
SRCA	Spectroradiometric Calibration Assembly
SV	Space View
SWINFRARED	Short Wavelength Infrared
TAC	Test Analysis Controller
TBD	to be determined
TDI	Time Delay Integration
TLCF	Team Leader Computing Facility
TM	Thematic Mapper
TOA	Top of the Atmosphere
TRMM	Tropical Rainfall Measuring Mission
TV	Thermal Vacuum
USGCRP	U.S. Global Change Research Program
VIS	Visible

9. APPENDIX E: REFERENCES

Abel, P., B. Guenther, R. Galimore, and J. Cooper, Calibration results for NOAA-11 AVHRR channels 1 and 2 from congruent ainfraredcraft observations, *J. Atmos. and Ocean. Technol., 10,* 493-508, 1993.

Barbieri, R., and B. Guenther, The MCST Management Plan, NASA Goddard Space Flight Center, Greenbelt MD, 1995.

Barker, J., J. Harnden, H. Montgomoery, P. Anuta, G. Kvaran, E. Knight, T. Bryant, A. McKay, J. Smid, and D. Knowles, MODIS Level 1 Geolocation, Characterization and Calibration Algorithm theoretical Basis Documnet, Version 1, Goddard Space Flight Center, Greenbelt MD, 1994.

Barnes, R., A. Holmes, W. Barnes, W. Esaias, and C. McClain, SeaWifs Prelaunch Radiometric Calibration and Spectral Characterization, NASA TM 104566, vol 23, October 1994.

Bremer, J., Optimization of the GOES-I Imager's radiometric accuracy: drift and 1/f noise suppression, *Optical Eng., 33* (10), 1994.

EOS, Functional and Performance Requinfraredements Specification for the Earth Observing System Data and Information System (EOSDIS) Core System, NASA, 1994.

Goldberg, I.L., Two-point calibration of non-linear PC HgCdTe channels, *Infrared Phys. Technol., 36,* 1995.

Guenther, B. ed. The MODIS Calibration Plan Version 2, GSFC, 1995.

Guenther, B., H. Montgomery, P. Abel, J. Barker, W. Barnes, P. Anuta, J. Baden, L. Carpenter, E. Knight, G. Godden, M. Hopkins, M. Jones, D. Knowles, S. Sinkfield, B. Veiga, N. Che, L. Goldberg, M. Maxwell, T. Zukowski, T. Pagano, N. Therrien, and J. Young, MODIS Level 1B Algorithm Theoretical Basis Document [MOD-02], GSFC, Greenbelt Maryland, 1995.

Guenther, B., W. Barnes, E. Knight, J. Barker, J. Harnden, G. Godden, H. Montgomery, and P. Abel, MODIS Calibration: A Brief Review of the Strategy for the At-Launch Calibration Approach, *J. Atmos Ocean. Tech., 13, 274-285,* 1996.

Hopkins, M., J. Baden, and J. Hannon, MODIS Level 1B Data Product Format, General Science Corporation, Seabrook MD, 1995a.

Hopkins, M., J. Hannon, and J. Baden, MODIS Level 1B Software Design Document, General Sciences Corporation, Seabrook MD, 1995b.

Kieffer, H.H., and R.L. Widley, Spectrophotometry of the Moon for Calibration of Spaceborne Imaging Instruments, in *Lunar and Planetary Science Conference 23*, pp. 687-688, 1992.

Kieffer, H.H., and R.L. Widley, Establishing the Moon as a Spectral Radiance Standard, *J. Atmos Ocean. Tech., 13, 360-375,* 1996.

King, M., Letter to John Parslow of CSINFRAREDO, 6 January 1994.

King, M., W.P. Menzel, P. Grant, J. Myers, G.T. Arnold, S. Platnick, L. Gumley, S. Tsay, C. Moeller, M. Fitzgerald, K. Brown, and F. Osterwisch, Ainfraredborne Scanning Spectrometer for Remote Sensing of Cloud, Aerosol, Water Vapor and Surface Properties, *JAOT, submitted,* 1995.

Knowles, D., S.Y. Qiu, H. Montgomery, F. Chen, ATBD 1996 Thermal Calibration Algorithm: Detailed Support Document, MCST G031. Oct 1996, General Sciences Corporation, .

Kurucz, R.L., Solar Flux Atlas from 296 to 1300 nm, National Solar Observatory, 1984.

McClain, C.R., W. Esaias, W. Barnes, B. Guenther, D. Endres, S.B. Hooker, B.G. Mitchell, and R. Barnes, Calibration and Validation Plan for SeaWiFS, NASA TM 104566, Vol 3, September 1992.

Mehrten, J., MODIS EM Temperature Telemetry Equations & Limits, SBRC, 1995.

Pagano, T., Gain Coefficients for Radiometric Calibration: version 2, SBRC, 1993.

Parker, K., and E. Knight, MODIS Operations Concept Document, GSFC, Greenbelt MD, 1995.

Rao, Degradation of the visible and near-infrared channels of the advanced very high resolution radiometer on the NOAA-9 spacecraft: assessment and recommendations for corrections, NOAA, 1993.

Salomonson, V.V., Team Leader Working Agreement for MODIS between the EOS AM & PM Projects at Goddard Space Flight Center and the MODIS Science Team Leader, Vincent V. Salomonson, of Goddard Space Flight Center, Goddard Space Flight Center, Greenbelt MD, 1994.

SBRS, Operational In-Flight Calibrations Procedures, CDRL 404, Hughes Santa Barbara Research Center, Santa Barbara California, 1993.

SBRS, Moderate Resolution Imaging Spectroradiometer (MODIS) Program Calibration Management Plan, SBRC, Goleta, California, 1994a.

SBRS, SBRC Critical Design Review Vol. III, 1994b.

Seber, G.A.F., *Linear Regression Analysis*, Wiley, 1977.

Slater, P.N., S.F. Biggar, R.G. Holm, R.D. Jackson, Y. Mao, M.S. Moran, J.M. Palmer, and B. Tuan, Reflectance and Radiance Based Methods for the in-flight Absolute Calibration of Multispectral Sensors, *Remote sensing of Envinfraredonment*, *22*, 11-37, 1987.

Slater, P., B. Biggar, K. Thome, Gellman, D., and P. Spyak, Vicarious Radiometric Calibrations of EOS Sensors, *J. Atmos Ocean. Tech.*, 1996.

Team, M.S., M.C.S. Team, M.S.D.S. Team, S.B.R. Center, and U.S.G.S. (Flagstaff), The MODIS Calibration Plan Version 1.1, GSFC, 1994.

Veiga,R., H.Montgomery, and M. Jones, MODIS Solar Reflective Band CalibrationAlgorithm, MCST Ref. No. G028, September 1996.

Veiga, R., H. Montgomery, and M. Jones, Solar Diffuser and Solar Diffuser Stability Monitor In-Flight Calibration Algorithm Implementation, General Sciences Corporation, Seabrook Maryland, 1995.

Weber, S.R., Specification for the Moderate-Resolution Imaging Spectroradiometer (MODIS), GSFC, Greenbelt Maryland, 1993.

Wehrli, C. Extraterrestrial Solar Spectrum, World Radiation Center (WRC), Davos-Dorf, Swtzerland, WRCPublication No. 615, July 1985.

Wolfe, R., J. Storey, E. Masuoka, and A. Fleig, MODIS Level 1A Earth Location Algorithm Theoretical Basis Document, NASA Goddard Space Flight Center, Greenbelt MD, 1995.

Young, J. B., SRCA along track SBR Modeling/algorithm, PL3095-N4214, August 24, 1995.

Young, J. B., SRCA Spectral Calibration Methodology, PL3095-N04744, March 20, 1995.

10. APPENDIX F: LEVEL 1B OUTPUT FILE SPECIFICATION

The five types of metadata are Core, Archive, Product, Swath, and SDS. The Core, Archive and Product metadata are stored as global attributes and the Swath metadata is stored as Vdata. The SDS metadata is stored as Science Data Set (SDS) attributes. The standard core granule metadata is the same for the three resolutions: 250m, 500m, and 1000m.

Global Metadata

ECS Standard Core Granule Metadata Stored as One ECS PVL String in xoremetadata.0=Global Attribute	
Description	**Example**
SHORTNAME	"MOD02"
LONGNAME	"MODIS MCST 10/31/96, Level 1B Earth View data, Version 2"
SIZEMBECSDATAGRANULE	400 (Obtained from system at runtime)
EASTBOUNDINGCOORDINATE	40.000000
WESTBOUNDINGCOORDINATE	15.000000
NORTHBOUNDINGCOORDINATE	25.000000
SOUTHBOUNDINGCOORDINATE	10.000000
EXCLUSIONGRINGFLAG	"N"
GRINGPOINTLATITUDE	(25.000000, 20.000000, 10.000000, 15.000000)
GRINGPOINTLONGITUDE	(20.000000, 40.000000, 35.000000, 15.000000)
GRINGPOINTSEQUENCENO	(1, 2, 3, 4)
ORBITNUMBER	1234
RANGEBEGINNINGDATETIME	"2002-02-23T11:02:27.987654Z"
RANGEENDINGDATETIME	"2002-02-23T11:04:57.987654Z"
QAPERCENTINTERPOLATEDDATA	0
QAPERCENTOUTOFBOUNDSDATA	0
QAPERCENTMISSINGDATA	0
AUTOMATICQUALITYFLAG	"passed"
OPERATIONALQUALITYFLAG	"not being investigated"
SCIENCEQUALITYFLAG	"not being investigated"
QUALITYFLAGEXPLANATION	"not being investigated"
REPROCESSINGACTUAL	"processed once"
REPROCESSINGPLANNED	"no further update anticipated"
INPUTPOINTER	"L1A and Geolocation file name(s)"
ANCILLARYINPUTPOINTER	"Reflective.LUT, Emissive.LUT, sd.coeff.trend"
GRANULEPOINTER	"L1B_Gran (name of this output file from DSS)"
PROCESSINGHISTORYPOINTER	"ECS reserved, static, logical ID number,TBD, from PCF
OPERATIONMODE	"day"
MODISPRODUCTFILENAME	"L1B_Gran (name of this output file)"
PROCESSINGDATETIME	"2002-02-23T11:04:57.987654Z"
SPSOPARAMETERS	"The SPSO parameters (see database) for all data contained in this file"

The archive granule metadata is the same for the three resolutions: 250m, 500m, and 1000m.

MODIS Level 1B Archive Granule Metadata Stored as HDF ECS PVL in :archivemetadata.0=Global Attribute	
Description	**Example**
ALGORITHMPACKAGEACCEPTANCEDATE	"1997-01-01"
ALGORITHMPACKAGEMATURITYCODE	"pre-launch"
ALGORITHMPACKAGENAME	"MOD02V2"
ALGORITHMPACKAGEVERSION	"version 2"
INSTRUMENTNAME	"Moderate-Resolution Imaging SpectroRadiometer"
PLATFORMSHORTNAME	"EOS AM1"
PROCESSINGCENTER	"GSFC"
ROUTINEINSTRUMENTOPERATIONS	“Y” or “N”
CALIBRATIONDATAQUALITY	“good”, “marginal” OR “bad”
NADINFRAREDPOINTING	“Y” or “N”
MISSIONPHASE	“A&E” OR “post A&E”

The product granule metadata is the same for the three resolutions: 250m, 500m, and 1000m.

MODIS Level 1B Product Granule Metadata Stored as Native HDF Global Attributes		
Description	**Format**	**Example**
"Number of Scans"	Int32	203
"Number of Day mode scans"	Int32	203
"Number of Night mode scans"	Int32	0
"Incomplete Scans"	Int32	14
“Max Earth View Frames”	Int32	1354
“Static Uncertainties”	float(38)	(?,...,?)
"%Valid EV Observations"	float(38)	98.2,..., 87.1,..,46.0,...
"%Saturated EV Observations"	float(38)	1.4,..., 0.2,...,7.9,...
“Post Processing Indicates Bad data”	Int32(38)	1=True; 0=False
“Electronics Redundancy Vector”	Int64	One bit set to 0 for Side A or 1 for Side B, for each programmable component
“Reflective LUT Last Change Date”	string	“1997-02-28T00:00:00”
“Emissive LUT Last Change Date”	string	“1997-02-28T00:00:00”
“Focal Plane Set Point State”	Int8(4)	0=Running open loop 1=Set Point is 83 degrees 2=Set Point is 85 degrees 3=Set Point is 88 degrees

Level 1B HDF-EOS Swath Metadata
Format is PVL, minimum size is approximately 2000 bytes, content TBD

"Level 1B Swath Metadata" Written as Vdata with the Following Fields		
Field	**Type**	**Typical value**
Scan Number	int32	Range 1 to 100
Complete Scan Flag	int32	Complete=1, Incomplete=0
Scan Type	char 32	"D"=day, "N"=night, "M"=mixed, "O"=other
EV Sector Start Time	float 64	
Minfraredror Side	int32	1 or 2
Programmed_EV_Frames	int32	1514
EV_Frames	int32	1354
Nadinfrared_Frame_Number	int32	677
Latitude of Nadinfrared Frame	float	$-\pi/2$ to $\pi/2$ in radians
Longitude of Nadinfrared Frame	float	$-\pi$ to π in radians
Solar Azimuth of Nadinfrared Frame	float	-31460 to 31460 in 0.1 mrad
Solar Zenith of Nadinfrared Frame	float	0 to 31460 in 0.1 mrad
Latitude of Last Frame Away from Glint	float	$-\pi/2$ to $\pi/2$ in radians
Longitude of last Frame Away from Glint	float	$-\pi$ to π in radians
No. thermistor outliers	int32	Range 0 to 12
Bit QA Flags	int32	1=True; 0=False
Moon in SV Port	bit 0	
Spacecraft Maneuver	bit 1	
Sector Rotation	bit 2	
Negative Radiance Beyond Noise Level	bit 3	
PC Ecal on	bit 4	
PV Ecal on	bit 5	
SD Door Open	bit 6	
SD Screen Down	bit 7	
SRCA On	bit 8	
SDSM On	bit 9	
Outgassing	bit 10	
Instrument Standby Mode	bit 11	
Linear Emissive Calibration	bit 12	
DC Restore Change	bit 13	
BB/Cavity Temperature Differential	bit 14	
BB Heater On	bit 15	
Remaining 16 bits reserved for future use	bits 16 - 31	

The Science Data Set attributes are partitioned according to resolution

Dimension SDS 250m		
"Band_250M(Band_250M)"	NA	Band_250M = 2
Band_250M Attributes: band_names = “1, 2” radiance_scales = x.f, x.f radiance_offsets = x.f, x.f radiance_units = “Watts/m^2/μm/steradian” reflectance_scales = x.f, x.f reflectance _offsets = x.f, x.f reflectance _units = “1/steradian” corrected_counts_scales = x.f, x.f corrected_counts_offsets = x.f, x.f corrected_counts_units = “counts”		

Dimension SDS 500m		
"Band_500M(Band_500M)"	NA	Band_500M = 5
Band_500M Attributes: band_names = “3, 4, 5, 6, 7” radiance_scales = x.f, x.f, x.f, x.f, x.f radiance_offsets = x.f, x.f, x.f, x.f, x.f radiance_units = “Watts/m^2/μm/steradian” reflectance_scales = x.f, x.f, x.f, x.f, x.f reflectance _offsets = x.f, x.f, x.f, x.f, x.f reflectance _units = “1/steradian” corrected_counts_scales = x.f, x.f, x.f, x.f, x.f corrected_counts_offsets = x.f, x.f, x.f, x.f, x.f corrected_counts_units = “counts”		

Dimension SDS 1000m		
"Band_1KM_RefSB (Band_1KM_RefSB)"	NA	Band_1KM_RefSB = 15
Band_1KM_RefSB Attributes: band_names = “8, 9, 10, 11, 12, 13lo, 13hi, 14lo, 14hi, 15, 16, 17, 18, 19, 26” radiance_scales = x.f, x.f, x.f, x.f, x.f, x.f, x.f, x.f, x.f, x.f, x.f, x.f, x.f, x.f, x.f radiance_offsets x.f, x.f, x.f, x.f, x.f, x.f, x.f, x.f, x.f, x.f, x.f, x.f, x.f, x.f, x.f radiance_units = “Watts/m^2/μm/steradian” reflectance_scales = x.f, x.f, x.f, x.f, x.f, x.f, x.f, x.f, x.f, x.f, x.f, x.f, x.f, x.f, x.f reflectance _offsets = x.f, x.f, x.f, x.f, x.f, x.f, x.f, x.f, x.f, x.f, x.f, x.f, x.f, x.f, x.f reflectance _units = “1/steradian” corrected_counts_scales = x.f, x.f, x.f, x.f, x.f, x.f, x.f, x.f, x.f, x.f, x.f, x.f, x.f, x.f, x.f corrected_counts_offsets = x.f, x.f, x.f, x.f, x.f, x.f, x.f, x.f, x.f, x.f, x.f, x.f, x.f, x.f, x.f corrected_counts_units = “counts”		
“Band_1KM_Emissive(Band_1KM_Emissive)"	NA	Band_1KM_Emissive = 16
Band_1KM_Emissive Attributes: band_names = “20, 21, 22, 23, 24, 25, 27, 28, 29, 30, 31, 32, 33, 34, 35, 36” radiance_scales = x.f, x.f, x.f, x.f, x.f, x.f, x.f, x.f, x.f, x.f, x.f, x.f, x.f, x.f, x.f, x.f radiance_offsets = x.f, x.f, x.f, x.f, x.f, x.f, x.f, x.f, x.f, x.f, x.f, x.f, x.f, x.f, x.f, x.f radiance_units = “Watts/m^2/μm/steradian” corrected_counts_scales = x.f, x.f, x.f, x.f, x.f, x.f, x.f, x.f, x.f, x.f, x.f, x.f, x.f, x.f, x.f, x.f corrected_counts_offsets = x.f, x.f, x.f, x.f, x.f, x.f, x.f, x.f, x.f, x.f, x.f, x.f, x.f, x.f, x.f, x.f corrected_counts_units = “counts”		

Instrument and Uncertainty SDS 250m		
"EV_250_Aggr500_RefSB "	Unsigned Integer (16 bits)	16 bit scaled integer array of dimension (Band_250M, 20*nscans, 2*EV_frames)
EV_250_Aggr500_RefSB Attributes: long_name ="Earth View 250M Aggregate 500M Reflected Solar Bands Scaled Integers"		
"EV_250_Aggr500_RefSB _Uncert_Indexes"	Int8	8 bit integer array of dimension (Band_250M,20*nscans, 2*EV_frames)
EV_250_Aggr500_RefSB _Uncert_Indexes Attributes: long_name ="Earth View 250M Aggregate 500M Reflected Solar Bands Uncertainty Indexes"		

Instrument and Uncertainty SDS 500m		
"EV_500_RefSB "	Unsigned Integer (16 bits)	16 bit scaled integer array of dimension (Band_500M, 20*nscans, 2*EV_frames)
EV_500_RefSB Attributes: long_name ="Earth View 500M Reflected Solar Bands Scaled Integers"		
"EV_500_RefSB_Uncert_ Indexes"	Int8	8 bit integer array of dimension (Band_500M, 20*nscans, 2*EV_frames)
EV_500_RefSB _Uncert_ Indexes Attributes: long_name ="Earth View 500M Reflected Solar Bands Uncertainty Indexes"		

Instrument and Uncertainty SDS 1000m		
"EV_1000_RefSB "	Unsigned Integer (16 bits)	16 bit scaled integer array of dimension (Band_1KM_RefSB, 10*nscans, EV_frames)
EV_1000_RefSB Attributes: long_name ="Earth View 1KM Reflected Solar Bands Scaled Integers"		
"EV_1000_RefSB _Uncert_ Indexes"	Int8	8 bit integer array of dimension (Band_1KM_RefSB, 10*nscans, EV_frames)
EV_1000_RefSB _Uncert_ Indexes Attributes: long_name ="Earth View 1KM Reflected Solar Bands Uncertainty Indexes"		
"EV_1000_Emissive "	Unsigned Integer (16 bits)	16 bit scaled integer array of dimension (Band_1KM_Emissive, 10*nscans, EV_frames,)
EV_1000_Emissive Attributes: long_name ="Earth View 1KM Emissive Bands Scaled Integers"		
"EV_1000_Emissive _Uncert_ Indexes"	Int8	8 bit integer array of dimension (Band_1KM_Emissive, 10*nscans, EV_frames,)
EV_1000_Emissive _Uncert_ Indexes Attributes: long_name ="Earth View 1KM Emissive Bands Uncertainty Indexes"		

11. APPENDIX G: SPURIOUS RADIANCE CONTRIBUTION SOURCES SUMMARY

Nominal Scene	Cavity Emission Sources [$L_{emiss}(T_{cav})$]	Earth Scene Sources $L_{scene\_refl}(T_{scene})$	
Earth View	1) Earth Aperture Surround Emission scattered into FOV. Estimated to be **nil** from Cavity Scatter model.	Scene Scatter	2) MODIS fore-optics and aft-optics will scatter radiances according to scene contrast details. Near-Field and Far-Field scatter are **not included** in L1B algorithm
		Cavity Reflections	3) Potential spurious reflections from cavity surfaces and scan mirror edges. Estimated to be **nil**.
		Fold Mirror Scatter	4) Fold Mirror scatter of Earth scene viewed directly by the Fold Mirror. Estimated to be **nil.**
Space View	1) Space View Surround , Emission scattered into FOV. Value estimation is in Ref	Cavity Reflections	2) Potential spurious reflections from cavity surfaces and scan mirror edges. Estimated to be **nil**.
		Fold Mirror Scatter	3) Fold Mirror scatter of Earth scene viewed directly by the Fold Mirror. Estimated to be **nil**.
Blackbody View	1) Cavity emission scattered via Scan Mirror into FOV. 2) Cavity emission reflected via blackbody into FOV	BB Reflections of Scene	2) Two distinct BB specular reflection paths from two localized Earth scene regions (+33º; -58º from nadir), and whole scene reflection paths from BB teeth imperfection.
		Cavity Reflections	3) Potential spurious reflections from cavity surfaces and scan mirror edges Estimated to be **nil**.
		Fold Mirror Scatter	4) Fold Mirror scatter of Earth scene viewed directly by the Fold Mirror. Estimated to be **nil**.